Author contributions

Y.O. conceived, designed, performed and analysed data from all experiments, and wrote the paper. S.T. and E.W. characterized R cells as mast-like cells *in vivo* and *in vitro* by flow cytometry, histo-cytochemical staining, electron microscopy, proliferation assays and microarray analyses, and edited the manuscript. S.S. and S.O performed immunoblotting, immunoprecipitation assays, *in vitro* GST-pulldown assays and RNA interference experiments. H.E. advised on the design of the *in vitro* experiments and edited the manuscript. R.A. conceived and supervised the project, analysed data and wrote the manuscript.

Additional information

Supplementary Information accompanies this paper at http://www.nature.com/naturecommunications

Competing financial interests: The authors declare no competing financial interests.

Reprints and permission information is available online at http://npg.nature.com/reprintsandpermissions/

How to cite this article: Obata, Y. *et al.* Oncogenic Kit signals on endolysosomes and endoplasmic reticulum are essential for neoplastic mast cell proliferation. *Nat. Commun.* 5:5715 doi: 10.1038/ncomms6715 (2014).

⌘ *Author's Choice*

THE JOURNAL OF BIOLOGICAL CHEMISTRY VOL. 289, NO. 30, pp. 20813–20823, July 25, 2014

Epidermal Growth Factor Receptor (EGFR) Signaling Regulates Global Metabolic Pathways in EGFR-mutated Lung Adenocarcinoma*[S]

Received for publication, April 21, 2014, and in revised form, June 9, 2014 Published, JBC Papers in Press, June 13, 2014, DOI 10.1074/jbc.M114.575464

Hideki Makinoshima[‡1], **Masahiro Takita**[‡§], **Shingo Matsumoto**[‡¶], **Atsushi Yagishita**[‡], **Satoshi Owada**[‖], **Hiroyasu Esumi**[‖], **and Katsuya Tsuchihara**[‡§]

From the [‡]*Division of Translational Research, Exploratory Oncology Research & Clinical Trial Center, National Cancer Center, Kashiwa, Chiba 277-8577, Japan,* [§]*Department of Integrated Biosciences, Graduate School of Frontier Sciences, The University of Tokyo, Kashiwa, Chiba 277-8561, Japan,* [¶]*Thoracic Oncology Division, National Cancer Center Hospital East, Kashiwa, Chiba 277-8577, Japan, and* [‖]*Research Institute for Biomedical Sciences, Tokyo University of Science, Noda, Chiba 278-0022, Japan*

Background: Genetic mutations in cancer-driver genes induce specific metabolic alterations in cancer cells.
Results: EGF receptor signaling has an important role for glycolysis, pentose phosphate pathway, and pyrimidine biosynthesis in EGFR-mutated lung cancer.
Conclusion: Our work reveals the relationship between the EGFR signaling axis and key metabolic changes.
Significance: These data implicate a possible link between therapeutic response and regulation of metabolism in EGFR-mutated LAD.

Genetic mutations in tumor cells cause several unique metabolic phenotypes that are critical for cancer cell proliferation. Mutations in the tyrosine kinase epidermal growth factor receptor (EGFR) induce oncogenic addiction in lung adenocarcinoma (LAD). However, the linkage between oncogenic mutated EGFR and cancer cell metabolism has not yet been clearly elucidated. Here we show that EGFR signaling plays an important role in aerobic glycolysis in EGFR-mutated LAD cells. EGFR-tyrosine kinase inhibitors (TKIs) decreased lactate production, glucose consumption, and the glucose-induced extracellular acidification rate (ECAR), indicating that EGFR signaling maintained aerobic glycolysis in LAD cells. Metabolomic analysis revealed that metabolites in the glycolysis, pentose phosphate pathway (PPP), pyrimidine biosynthesis, and redox metabolism were significantly decreased after treatment of LAD cells with EGFR-TKI. On a molecular basis, the glucose transport carried out by glucose transporter 3 (GLUT3) was downregulated in TKI-sensitive LAD cells. Moreover, EGFR signaling activated carbamoyl-phosphate synthetase 2, aspartate transcarbamylase, and dihydroorotase (CAD), which catalyzes the first step in *de novo* pyrimidine synthesis. We conclude that EGFR signaling regulates the global metabolic pathway in EGFR-mutated LAD cells. Our data provide evidence that may link therapeutic response to the regulation of metabolism, which is an attractive target for the development of more effective targeted therapies to treat patients with EGFR-mutated LAD.

The discovery of oncogenic driver mutations allows us to identify druggable targets and develop new therapies using small molecule tyrosine kinase inhibitors (TKIs)[2] aimed at the relevant patient populations (1–3). More than 50% of lung adenocarcinomas (LAD) from East Asian non-smokers harbor EGFR mutations, and these tumors have been termed oncogene addicted to reflect their dependence on EGFR-mediated pro-survival signaling and their high susceptibility to apoptosis induced by EGFR-TKIs (*e.g.* gefitinib and erlotinib) (4–7). The tyrosine kinase activity of EGFR is dysregulated by gene mutations that lead to aberrant EGFR signaling through pathways including the RAS/MAPK and PI3K/AKT pathways (8, 9). The most frequently occurring mutations in the *EGFR* gene (in-frame deletion in exon 19 at codons 746–750 or a single-base substitution L858R in exon 21) predict an improved clinical response to first-line oral EGFR-TKIs compared with standard platinum-based chemotherapy in patients with advanced non-small-cell lung carcinoma (NSCLC) (4, 8).

There is accumulating evidence that genetic mutations in cancer-driver genes, tumor suppressors, and amplified oncogenes are linked to specific alterations in metabolic activity in cancer cells, involving proteins such as isocitrate dehydrogenase (IDH), fumarate hydratase (FH), MYC, K-RAS, and BRAF (10–13). The Warburg effect, the phenomenon in which cancer cells exhibit rapid glucose consumption with secretion of lactate despite abundant oxygen availability, has been recognized since the 1930s (14–16). Indeed, glucose metabolism in cancer cells is tightly regulated by many molecules at the transcriptional, translational, and post-translational levels (10, 17, 18). c-MYC is critically involved in the regulation of many growth-

* This work was supported by the National Cancer Center Research and Development Fund (25-A-6) and JSPS KAKENHI Grant Number 24300345 (to K. T.).
[S] This article contains supplemental Tables S1 and S2.
⌘ *Author's Choice*—Final version full access.
[1] To whom correspondence should be addressed: Division of Translational Research, Exploratory Oncology Research & Clinical Trial Center, National Cancer Center, Kashiwa, Chiba 277-8577, Japan. Tel.: 81-4-7134-6855; Fax: 81-4-7134-6865; E-mail: hmakinos@east.ncc.go.jp.

[2] The abbreviations used are: TKI, tyrosine kinase inhibitor; EGFR, epidermal growth factor receptor; LAD, lung adenocarcinoma; IC_{50}, half maximal inhibitory concentration; PPP, pentose phosphate pathway; ECAR, extracellular acidification rate; OCR, oxygen consumption rate; GLUT, glucose transporter; CAD, carbamoyl-phosphate synthetase 2, aspartate transcarbamylase, and dihydroorotase.

promoting signal transduction pathways and glucose metabolism genes, including GLUT1, hexokinase 2 (HK2), pyruvate kinase muscle (PKM2), and lactate dehydrogenase A (LDHA) (10, 19). Through the up-regulation of these genes, c-MYC contributes directly to the Warburg effect (19). The enzymatic activities of glycolytic enzymes such as HK2, phosphofructokinase (PFK), PKM2, and LDHA are modulated by post-translational modification (18). For example, PKM2 is phosphorylated in its tyrosine residue (Y105) with low activity in human cancer cells, resulting in increased lactate production, which is one-step downstream from PKM2 in glycolysis, even under aerobic conditions (14, 17). Furthermore, PKM2 promotes the Warburg effect through EGF-stimulated EGFR activation and the MAPK signaling pathway (20, 21). In brain cancer, the activating EGFRvIII mutation induces enhanced glycolysis by promoting glycolytic gene expression through the Myc/Max pathway (22). However, the specific role of mutated EGFR for aerobic glycolysis in lung cancer has not yet been clearly described.

In this work, we demonstrate that EGFR signaling is required for lactate production under aerobic growth conditions in LAD cells. EGFR signaling maintains key metabolites in glycolysis and PPP by regulating glucose transport through GLUT3 expression. In addition to glucose metabolism, we show that EGFR signaling up-regulates *de novo* pyrimidine biosynthesis. Moreover, we describe the altered metabolic profiles in TKI-sensitive LAD cells in response to erlotinib. Our results imply that EGFR signaling plays a central role in modulating global metabolic pathways in EGFR-mutated LAD.

EXPERIMENTAL PROCEDURES

Materials—Cell lines were purchased from the Immuno-Biological Laboratories (Fujioka, Japan) and American Type Culture Collection (ATCC). RPMI 1640 (R8758 and R1383), phosphate-buffered saline (PBS), 2-deoxy-D-glucose (2DG) were purchased from Sigma-Aldrich. Fetal bovine serum (FBS) was purchased from Biowest (Nuaille, France). Dimethyl sulfoxide (DMSO) and glucose were purchased from Wako Pure Chemicals Industries (Osaka, Japan). Gefitinib and erlotinib were purchased from Santa Cruz Biotechnology (Dallas, TX). Cell Counting Kit-8 was purchased from Dojindo Laboratories (Kumamoto, Japan). Lactate assay kit II and glucose assay kit II were purchased from BioVision (Milpitas). FluxPak XF24 assay pack and XF glycolysis stress test kit were purchased from Seahorse Bioscience (North Billerica). Countess Automated Cell Counter including Trypan Blue and chamber slides was purchased from Invitrogen (Carlsbad, CA). Primary antibodies specific for EGFR, phospho-EGFR Tyr-1068, AKT, phospho-AKT Ser473, ERK1/2, phospho-ERK1/2 Thr202/Tyr204, GSK3α/β, phospho-GSK3α/β Ser21/9, c-MYC, PKM2, phospho-PKM2 Tyr105, GYS, phospho-GYS Ser641, LDHA, phospho-LDHA Tyr-15, HK2, S6K, phospho-S6K Thr421/Ser424, CAD, phospho-CAD (Ser-1859), and β-actin were purchased from Cell Signaling Technologies (Danvers, MA) and GLS, GLUT1, GLUT3, PDHA1, and phospho-PDHA1 Ser-293 from Abcam (Cambridge, UK), respectively. The peroxidase-linked secondary antibodies for WB, HRP-linked Sheep anti-mouse IgG and Donkey anti-rabbit IgG, were purchased from GE Healthcare Biosciences (Pittsburgh, PA). Fluorescein (FITC)-conjugated goat anti-rabbit IgG for FACS was purchased from Beckman Coulter (Fullerton, CA). Oligomycin was purchased from Merck Millipore (Darmstadt, Germany). SYBR Premix Ex Taq was purchased from TaKaRa Bio (Shiga, Japan). Ribonuclease A (RNase A) was purchased from Roche Applied Science (Penzberg, Germany) and contaminated DNase was inactivated at 80 °C for 30 min. 3-*O*-(^{3}H-methyl)-*D*-glucose (3-OMeG) was purchased from Perkin Elmer (Waltham, MA).

Cell Survival Assay and Proliferation Assay—EGFR mutant LAD cells were seeded in RPMI 1640 containing various concentrations of EGFR inhibitors in 96-well cell culture plates. After 72 h of incubation, cell viability was analyzed using a WST-8 assay using the Cell Counting Kit-8 (Dojindo, Japan). To count the number of viable cells, Trypan Blue-negative cells were counted using a Countess Automated Cell Counter (Invitrogen).

Lactate and Glucose Assay—Lactate and glucose in culture medium were measured with the respective lactate assay kit II and glucose assay kit II according to the manufacturer's instructions (BioVision, Mountain View, CA). Briefly, after centrifugation (3,500 rpm, 15 min, 4 °C), cell culture medium supernatants were frozen at −20 °C. Samples were later thawed, diluted in assay buffer, and mixed with lactate or glucose reaction mixture for 30 min. The optical density of the mixture in each well was read at 450 nm on a microplate reader (Molecular Devices). The lactate concentration was calculated from a standard curve and normalized to cell numbers and culture time. Glucose consumption was calculated from a standard curve, subtracting background from cell-free medium, and normalizing to cell numbers and time.

Measurement of ECAR and OCR—ECAR and OCR were measured with a XF glycolysis stress test kit according to the manufacturer's instructions (Seahorse Bioscience). In brief, 4.5×10^4 cells were plated onto XF24 plates in RPMI 1640 (10% FBS, 2 mM glutamine) and incubated at 37 °C, 5% CO_2 overnight. Cells were washed with assay medium (minus glucose and unbuffered RPMI 1640 (SIGMA R1383)), replaced with assay medium, and then placed at 37 °C in a CO_2-free incubator for 30 min. ECAR and OCR were monitored using a Seahorse Bioscience XF24 Extracellular Flux Analyzer over time and each cycle consisted of 3 min mixing, 3 min waiting and 3 min measuring. Glucose, oligomycin, and 2DG were diluted into XF24 media and loaded into the accompanying cartridge to achieve final concentrations of 10 mM, 5 μM, and 100 mM, respectively. Injections of the drugs into the medium occurred at the time points specified.

Western Blotting—Cells were lysed in RIPA buffer (150 mM NaCl, 1% Triton X-100, 0.5% sodium deoxycholate, 0.1% SDS, 50 mM Tris, pH 8.0) on ice for 10 min, sonicated, and centrifuged at 15,000 × *g* for 10 min. The protein content of supernatants was measured by BCA assay (Pierce). Identical amounts of protein samples were separated via 4–20% SDS/PAGE, transferred to PVDF membranes, and incubated overnight with primary antibodies (1:1000 dilution). The primary antibodies used in this study are listed in the materials. ECL anti-rabbit IgG HRP-linked whole antibody (1:10,000; GE Healthcare) and ECL anti-mouse IgG HRP-linked whole antibody (1:10,000; GE Healthcare) were used as secondary antibodies. Signals were

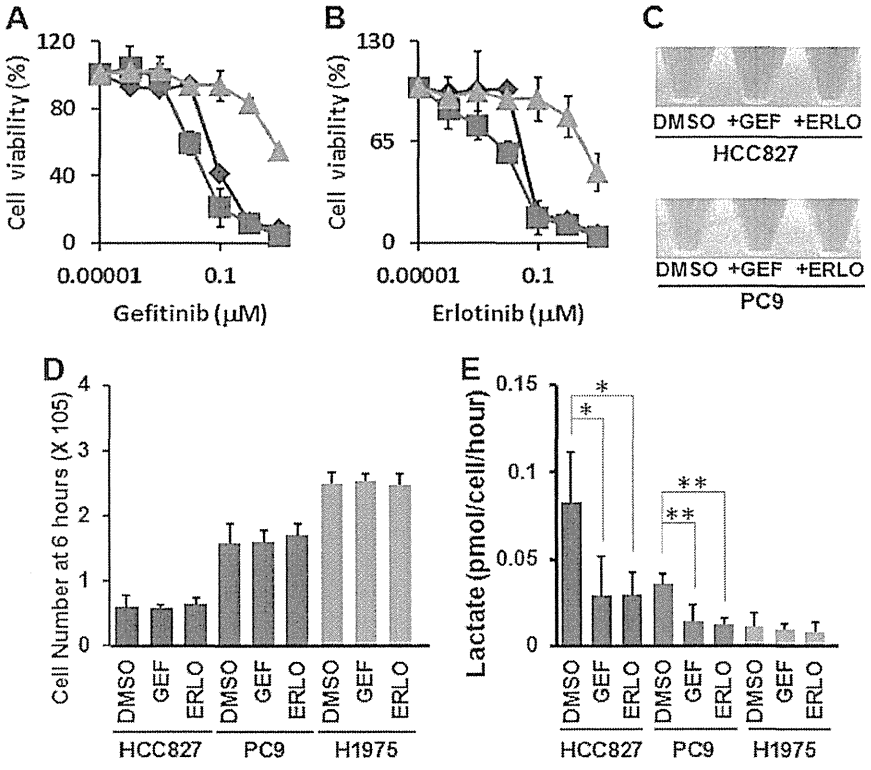

FIGURE 1. **EGFR-TKI treatment represses lactate production in TKI-sensitive LAD cells.** *A*, WST-8 assay with gefitinib. Cells were treated with the indicated inhibitors for 72 h, and the viability was assessed by the WST-8 assay. Data are shown as the mean ± S.D. ($n = 6$). *Blue line*: HCC827, *red line*: PC-9, *green line*: H1975. The *in vitro* half-maximal inhibitory concentration (IC_{50}) for the growth of EGFR-mutated LAD cell lines was determined such that HCC827 to gefitinib: 0.085 μM, PC-9 to gefitinib: 0.031 μM, and H1975 to gefitinib: >10 μM. *B*, WST-8 assay with erlotinib. Cells were treated with the indicated concentrations for 72 h, and viability was assessed by the WST-8 assay. The data are shown as the mean ± S.D. ($n = 6$). *Blue line*: HCC827, *red line*: PC-9, *green line*: H1975. The *in vitro* half-maximal inhibitory concentration (IC_{50}) for the growth of EGFR-mutated LAD cell lines was determined such that HCC827 to 0.065 μM, PC-9 to 0.067 μM and H1975 to 8.8 μM. *C*, medium color in HCC827 and PC-9 was altered by addition of EGFR-TKIs (1 μM) for 24 h. The phenol red in culture media exhibits a gradual color transition from red to yellow over the pH range 8.0 to 6.6. *D*, cell growth responses at 6 h to 1 μM of gefitinib or erlotinib were measured using a Trypan Blue staining. The cell number of HCC827 (*blue*), PC-9 (*red*), and H1975 were shown. GEF; gefitinib, ERLO; erlotinib. The data are shown as the mean ± S.D. ($n = 4$). *, $p < 0.05$; **, $p < 0.01$ *versus* control by two-tailed Student's *t* test. *E*, extracellular lactate production in HCC827 (*blue*), PC-9 (*red*) and H1975 (*green*) cell lines at 6 h post-TKI treatment. Error bars indicate S.D. ($n = 6$). *, $p < 0.05$; **, $p < 0.01$ *versus* control by two-tailed Student's *t* test.

detected using ECL Western blotting detection reagent (GE Healthcare) and x-ray films (GE Healthcare).

Quantitative RT-PCR—Cells were washed with PBS and total RNA from the LAD cell lines was isolated with TRIzol Reagent (Invitrogen). Complementary DNA (cDNA) was synthesized using the SuperScript VILO cDNA synthesis kit (Invitrogen). Synthesized primers were purchased from TaKaRa Bio (Japan). Real-time RT-PCR was carried out with specific primers and a 7500 detection system (Applied Biosystems). β-Actin was used for normalization as control and the relative quantitation value compared with the calibrator for that target is expressed as $2^{-(Ct-Cc)}$.

Metabolite Measurements—Metabolic extracts were prepared from 2–5 × 10^6 cells with methanol containing Internal Standard Solution (Human Metabolome Technologies; HMT, Inc., Tsuruoka, Japan) and analyzed using a capillary electrophoresis (CE)-connected ESI-TOFMS and CE-MS/MS system (HMT, CARCINOSCOPE). 2–5 × 10^6 cells were used for the extraction of intracellular metabolites. Culture medium was removed from the dish, and cells were washed twice in 5% mannitol solution (10 ml first and then 2 ml). Cells were then treated with 800 μl of methanol and 550 μl of Milli-Q water containing internal standards (H3304–1002, HMT, Inc., Tsuruoka, Japan). The metabolite extract was transferred into a microfuge tube and centrifuged at 2,300 × *g* and 4 °C for 5 min. Next, the upper aqueous layer was centrifugally filtered through a Millipore 5-kDa cutoff filter at 9,100 × *g* and 4 °C for 120 min to remove proteins. The filtrate was centrifugally concentrated and resuspended in 50 μl of Milli-Q water for CE-MS analysis. Cationic compounds were analyzed in the positive mode of CE-TOFMS and anionic compounds were analyzed in the positive and negative modes of CE-MS/MS according to the methods developed by Soga *et al.* (23–25). To obtain peak information including *m/z*, migration time (MT), and peak area, detected peaks by CE-TOFMS and CE-MS/MS were extracted using automatic integration software (MasterHands, Keio University, Tsuruoka, Japan and MassHunter Quantitative Analysis B.04.00, Agilent Technologies, Santa Clara, CA, respectively). The peaks were annotated with putative metabolites from the HMT metabolite database based on their MTs in CE and *m/z* values determined by TOFMS. The tolerance range for the peak annotation was configured at ±0.5 min for MT and ±10 ppm for *m/z*. In addition, concentrations of metabolites were calculated by normalizing the peak area of each metabolite with respect to the area of the internal standard and by using standard curves, which were obtained by three-point calibrations.

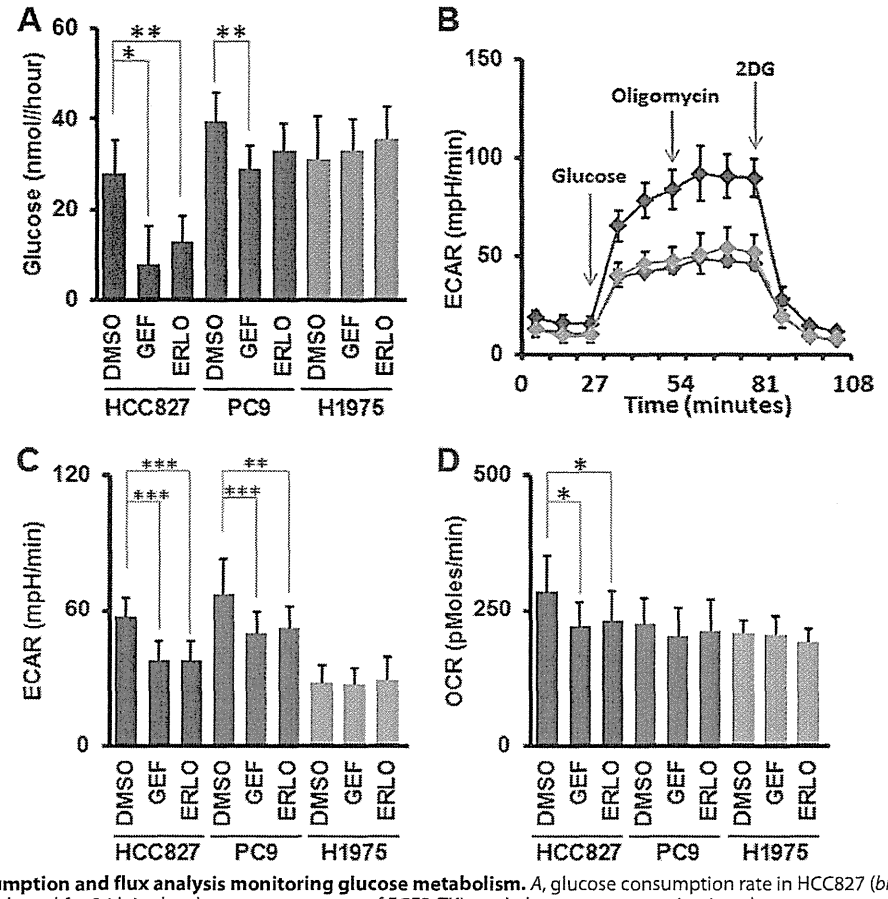

FIGURE 2. **Glucose consumption and flux analysis monitoring glucose metabolism.** *A*, glucose consumption rate in HCC827 (*blue*), PC-9 (*red*), and H1975 (*green*) cells. Cells were cultured for 24 h in the absence or presence of EGFR-TKIs and glucose concentration in culture supernatant was quantified. Cell-free medium was used as a background control. Error bars indicate S.D. ($n = 6$). *, $p < 0.05$; **, $p < 0.01$ *versus* control by two-tailed Student's *t* test. *B*, measurement of ECAR over time. After 6-h treatment with TKIs, cells were applied to flux assay. ECAR was measured every 9 min. The addition of glucose, oligomycin, and 2-deoxy-D-glucose (*2DG*) was carried out at the time point indicated by the *arrows*. Error bars indicate S.D. C, ECAR values of HCC827 (*blue*), PC-9 (*red*), and H1975(*green*) cells at 36 min of flux assay. Error bars indicate S.D. ($n = 24–30$). **, $p < 0.005$; ***, $p < 0.001$ *versus* control by two-tailed Student's *t* test. All cells were treated with the indicated TKIs (1 μM) for 6 h before each assay. *GEF*, gefitinib; *ERLO*, erlotinib. *D*, OCR values of HCC827 (*blue*), PC-9 (*red*), and H1975 (*green*) cells at 36 min of flux assay. Error bars indicate S.D. ($n = 24–30$). *, $p < 0.001$ *versus* control by two-tailed Student's *t* test. All cells were treated with the indicated TKIs (1 μM) for 6 h before each assay. *GEF*, gefitinib; *ERLO*, erlotinib.

Expression of Glucose Transporter and Glucose Transport Assay—To detect expression of membrane-bound GLUTs, cells were fixed with 80% ethanol and incubated with anti-GLUT3 antibody (Abcam) and stained with the appropriate FITC-conjugated anti-rabbit IgG antibody (Jackson Immuno Research). Quantification of FITC-fluorescent intensity was performed using a FACSCanto II (BD Biosciences). Procedures for 3-OMeG uptake assay were previously described (26). LAD cells were treated with indicated TKIs for 6 h before glucose transport assay. Uptake was performed from 0.5 min to 10 min and radioactivity in the cells was quantified with Tri-Carb 3110TR low activity liquid scintillation analyzer (PerkinElmer).

Statistical Analyses—Unless otherwise indicated, results were reported as the mean ± S.D. Statistical analyses were done by two-tailed Student's *t* test. For metabolomic data analysis we used Welch *t* test and *p* values were indicated as *, <0.05; **, <0.01; and ***, <0.001.

RESULTS

Lactate Production Was Decreased in TKI-sensitive LAD Cells after EGFR-TKI Treatment—We initially characterized the EGFR-mutated lung adenocarcinoma cell lines used in this study by measuring cell viability in the absence or presence of EGFR-TKIs after 72 h. All three LAD cell lines have the EGFR mutation in either exon 19 or exon 21. Cell line HCC827 carried the delE746-A750 mutation, PC-9 exhibited delE746-A750 and NCI-H1975 (H1975) carried EGFR L858R+T790M (27, 28). The H1975 cells have the T790M mutation, which causes resistance to gefitinib and erlotinib (29). HCC827 and PC-9 cell lines were highly sensitive to the EGFR-TKI gefitinib and erlotinib in the nanomolar range as compared with the TKI-resistant cell H1975 (Fig. 1, *A* and *B*). These data are consistent with previous findings (27, 28, 30).

In dose response assays with EGFR inhibitors, we observed differences in the color of the culture medium in the presence of TKIs against EGFR, especially in the growth cultures of TKI-sensitive cell lines (Fig. 1*C*). In culture media, phenol red exhibits a gradual color transition from red to yellow at lower pH values as a result of lactate production (31). Therefore, we explored the glycolytic capacity of EGFR-mutated LAD cells. Since a 72-h incubation with TKIs leads to a dramatic reduction in cell viability in sensitive cell lines, we set up experimental conditions where TKI treatment was given at a relatively higher concentration (1 μM) and

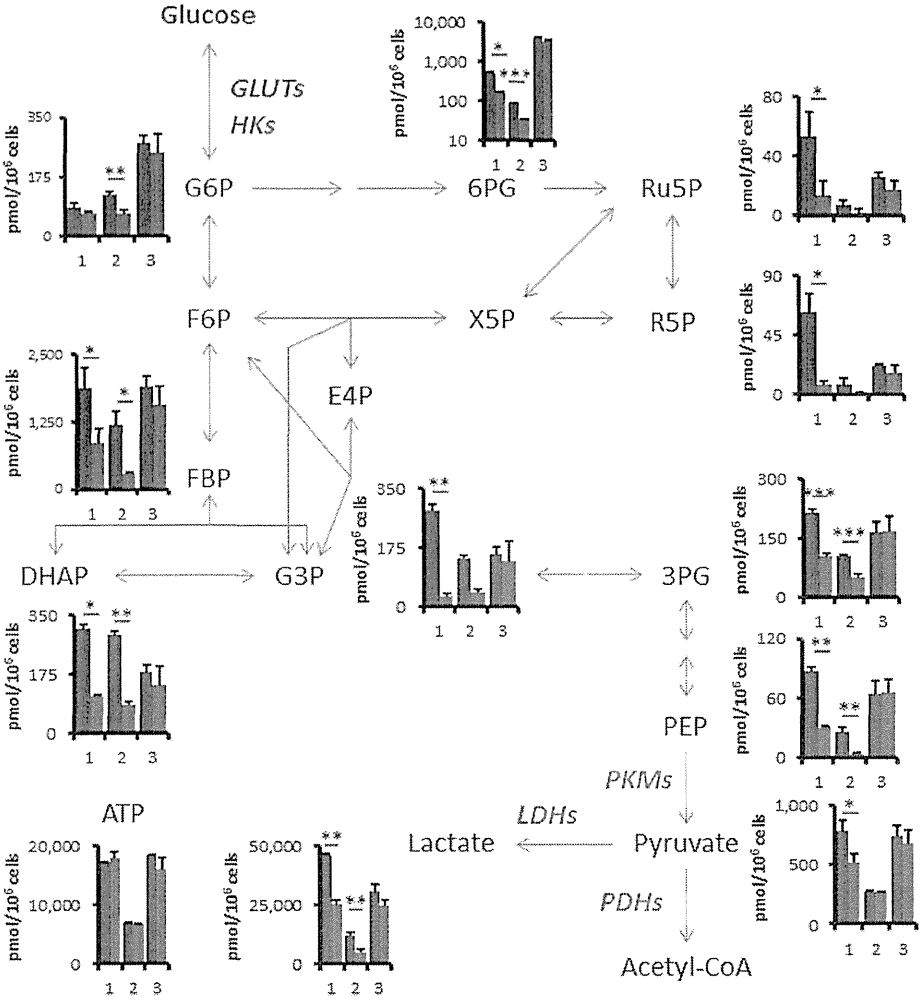

FIGURE 3. **EGFR signaling up-regulates glycolysis and the pentose phosphate pathway.** Intracellular concentration (pmol/million cells) of key metabolites involved in glycolysis and pentose phosphate pathway (*PPP*) after the inhibition of EGFR signaling is shown. Error bars indicate S.D. ($n = 3$). Total metabolites were extracted with methanol from HCC827, PC9 or H1975 cells treated with DMSO (*blue*) or erlotinib (*red*, 1 μM) for 6 h. Representative metabolites such as glucose 6-phosphate (*G6P*), fructose 1,6-bisphosphate (*FBP*), glyceraldehyde 3-phosphate (*G3P*), dihydroxyacetone phosphate (*DHAP*), 3-phosphoglycerate (*3PG*), phosphoenolpyruvate (*PEP*), pyruvate (*PA*), lactate (*LA*), 6-phosphogluconate (*6PG*), ribulose 5-phosphate (*Ru5P*), ribose 5-phosphate (*R5P*), and ATP are shown here. Others are listed in supplemental Table 1.

shorter time (6 h) to allow all cells to grow equally and thereby standardize the number of viable cells analyzed (Fig. 1*D*). Interestingly, we discovered that exposure of the cells to TKIs for up to 6 h significantly lowered the rate of lactate accumulation in the medium of TKI-sensitive LAD cell lines but not in resistant cells (Fig. 1*E*, *, $p < 0.05$; **, $p < 0.01$ *t* test).

Glycolytic Activities Were Down-regulated in TKI-sensitive LAD Cells after Inhibition of EGFR Signaling—Next, we quantified the glucose consumption rate and found that inhibition of EGFR signaling significantly lowered the rate of glucose consumption from the growth medium of TKI-sensitive HCC827 and PC9 cells but not in the TKI-resistant H1975 cells (Fig. 2*A* *, $p < 0.05$; **, $p < 0.01$ *t* test).

To better define lactate production derived from glucose, we measured the glucose-induced extracellular acidification rate (ECAR), an indicator of lactate production, and the oxygen consumption rate (OCR), an indicator of oxidative phosphorylation (OXPHOS), using a flux analyzer. Basal levels of ECAR at the beginning of measurements, which indicated non-glycolytic acidification, were low in HCC827 cells (Fig. 2*B*). Equivalent ECAR was observed in HCC827 cells both pre- and post-treatment with an ATPase inhibitor oligomycin to induce maximum cellular glycolytic capacity (Fig. 2*B*). At the final step, the addition of 2-deoxy-D-glucose (2DG), an inhibitor for glycolysis, completely shut down extracellular acidification (Fig. 2*B*). ECAR was statistically higher in DMSO controls compared with TKI-treated HCC827 and PC-9 cells (Fig. 2*C* *, $p < 0.01$; **, $p < 0.005$; ***, $p < 0.001$ *t* test). In contrast to ECAR, OCR was changed in TKI-treated HCC827, but not in PC-9 and H1975 cells (Fig. 2*D*).

EGFR Signaling Up-regulates Glycolysis and the Pentose Phosphate Pathway—To confirm the reduction of glycolysis metabolites by TKIs, we extracted intracellular metabolites with methanol and analyzed using capillary electrophoresis time-of-flight mass spectrometry (CE-TOFMS) (25). Metabolome analysis revealed that intermediate metabolites in glycolysis and the pentose phosphate pathway (PPP) were down-regulated by erlotinib treatment for 6 h in both HCC827 and PC-9

cells (Fig. 3 and supplemental Table S1). We observed that key glycolysis and PPP metabolites such as fructose 1,6-bisphosphate (FBP), dihydroxyacetone phosphate (DHAP), 3-phosphoglycerate (3PG), phosphoenolpyruvate (PEP), lactate (LA), and 6-phosphogluconate (6PG) were decreased in TKI-sensitive HCC827 and PC9 cells after 6 h of erlotinib treatment, but not in TKI-resistant H1975 cells (Fig. 3 and supplemental Table S1). Glucose 6-phosphate (G6P), glyceraldehyde 3-phosphate (G3P), pyruvate (PA), ribulose 5-phosphate (Ribu5P), and ribose 5-phosphate (R5P) were significantly reduced in both HCC827 and PC9 cells. The amount of adenosine triphosphate (ATP), which is the molecular unit of currency of intracellular energy transfer, was not changed in any of the tested three cell lines after erlotinib treatment. The reduction of glucose utilization after TKI treatment was observed in both glycolysis and pentose phosphate pathways, suggesting that EGFR signaling might regulate a glucose transport or hexokinase activity in TKI-sensitive LAD cells.

MYC-regulated Gene Expression for Glycolytic Enzymes—To test whether EGFR-TKIs inhibited EGFR activity and related signaling molecules under our experimental conditions, we determined levels of total EGFR, phospho-EGFR (p-EGFR), ERK1/2, p-ERK1/2, AKT, p-AKT, MYC, and β-actin in cells treated with DMSO or gefitinib (1 μM) for 2 h by Western blot (WB) analyses. Despite equivalent amounts of total EGFR, p-EGFR was clearly repressed in HCC827 and PC9 cells, but not in H1975 cells (Fig. 4*A*). Downstream signaling molecules such as ERK1/2 and AKT were also inactivated by the addition of gefitinib to HCC827 and PC9 cells as compared with H1975 cells (Fig. 4*A*).

We hypothesized that MYC regulates lactate production through transcriptional regulation, since MYC is an important regulator for cell cycle and glycolysis in cancer cells (19, 32, 33). We found that the levels of MYC were quickly down-regulated at both the mRNA and protein levels in response to EGFR-TKIs (Fig. 4, *A* and *B*). The MYC-regulated genes GLUT1 (glucose transporter 1) and HK2 (Hexokinase 2) were down-regulated in EGFR-TKI sensitive LAD cells, but not in the TKI-resistant H1975 cells (Fig. 4, *C* and *D*). Although previous studies reported that MYC up-regulated PKM2 (pyruvate kinase muscle isozyme 2) (34), we found that the loss of MYC did not affect mRNA expression of PKM2 in HCC827 or PC9 cells (Fig. 4*E*). These data suggest that the reduction of glycolysis after the inhibition of EGFR signaling is caused by down-regulation of the MYC pathway.

Protein Expression and Phosphorylation of Metabolic Enzymes—PKM2 is thought to be a key molecule for aerobic glycolysis in cancer cells (20, 21). We hypothesized that PKM2 might play a critical role in the glycolysis pathway in the response to EGFR-TKI treatment, since PKM2 activity was down-regulated by EGF stimulation resulting in up-regulated lactate production (21). Although the phosphorylation of PKM2 at Tyr-105 was decreased at 24 h after EGFR-TKI addition in TKI-sensitive HCC827 and PC9 cells, this was not seen at the earlier time points (2 or 6 h) post-treatment (Fig. 5*A*). The phosphorylation of PKM2 was not changed in TKI-resistant H1975 cells over time (Fig. 5*A*). Therefore, there may be a more rapid, PKM2-

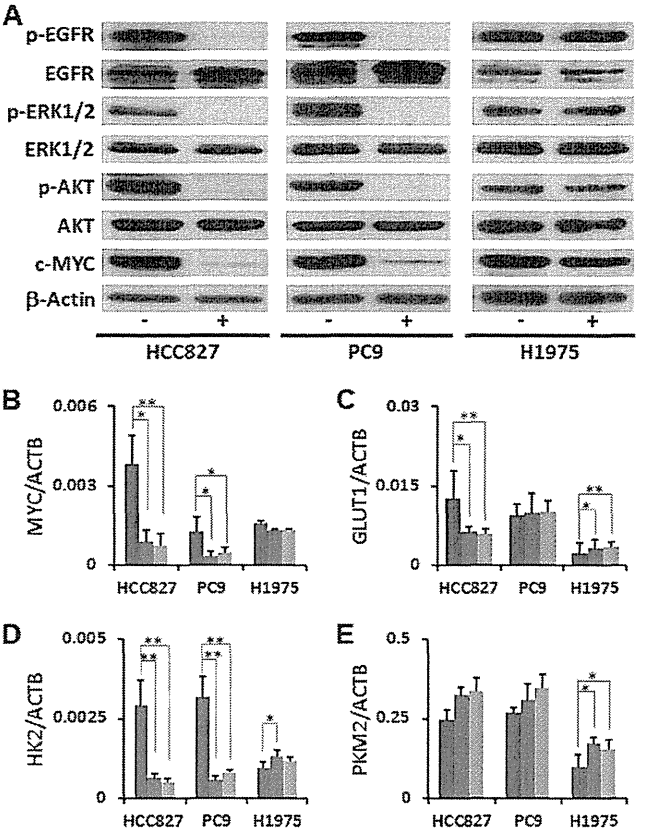

FIGURE 4. **MYC-regulated glycolytic gene expression.** *A*, Western blotting (*WB*) showing proteins related with EGFR signaling. EGFR, phospho-EGFR (*p-EGFR*), ERK1/2, phospho-ERK1/2 (*p-ERK1/2*), AKT, phospho-AKT (*p-AKT*) and c-MYC. Total protein lysates were isolated from the cell treated with gefitinib for 2 h. Equivalent amounts of proteins from whole-cell lysates were subjected to Western blot analysis to detect the indicated proteins. β-Actin was used as a loading control. *B-E*, total RNA was isolated from cells at 6 h post-TKI treatment and analyzed by RT-PCR. *Blue bars* represent DMSO control, *red bars* denote gefitinib treatment, and *green bars* denote erlotinib treatment. The representative genes related with glycolysis are shown here. *MYC*, *GLUT1* (glucose transporter 1, *SLC2A1*), *HK2* (hexokinase 2), and *PKM2* (pyruvate kinase muscle isozyme 2), and others were listed in supplemental Table S2. Error bars indicate S. D. ($n = 6$). *, $p < 0.05$; **, $p < 0.01$ *versus* control by two-tailed Student's *t* test.

independent molecular mechanism by which EGFR signaling regulates the glycolysis pathway.

To determine whether the changes in gene expression driven by MYC were associated with modifications of cellular metabolism, we analyzed phosphorylation and expression of EGFR signaling molecules and glycolytic enzymes by Western blot. We confirmed the effect of TKIs on molecular markers of the EGFR signaling cascade (EGFR, AKT, ERK, and c-Myc) in LAD cells incubated in the presence of gefitinib or erlotinib. We observed that phosphorylation of EGFR, AKT, and ERK was inhibited at 6 h after TKI treatment in HCC827 and PC9 cells (Fig. 5*B*). The expression level of enzymes for glucose metabolism such as GLUT1 and HK2 generally showed regulation in mRNA levels but not at the corresponding protein levels (Fig. 5*B*). In contrast, GLUT3 was decreased in HCC827 and PC-9 cells after 6 h treatment with TKIs (Figs. 4*C* and 5*B*). When we examined the expression level of MYC-regulated glutaminase (GLS) and glycogen synthase (GYS), we saw that GLS and p-GYS were modestly down-regulated in HCC827 and PC9

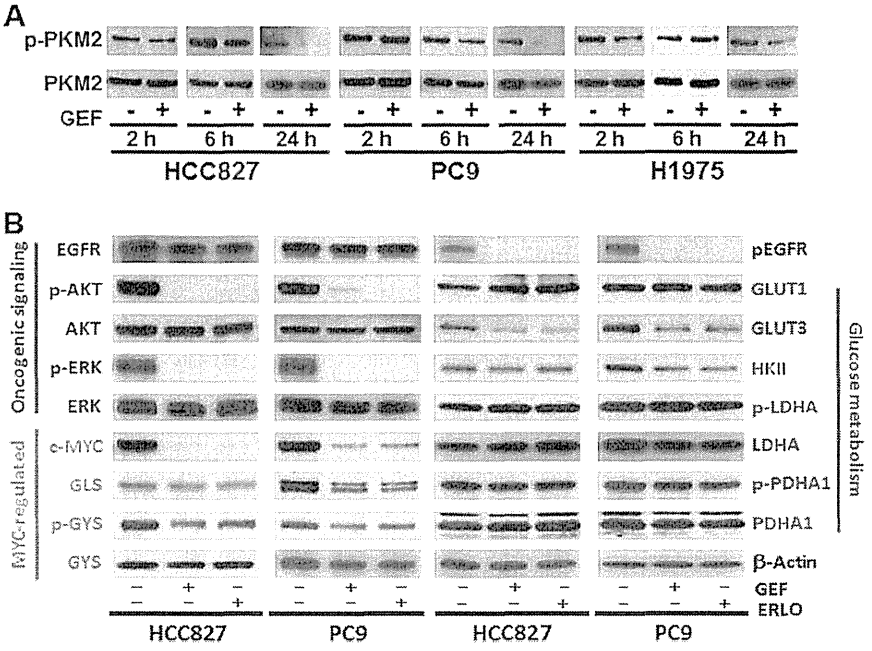

FIGURE 5. **Protein expression and phosphorylation of metabolic enzymes.** *A*, phosphorylation of PKM2 at Tyr-105 is decreased 24 h after EGFR-TKI addition. EGFR inhibition in the TKI-sensitive HCC827 and PC9 cells did not induce significant reduction of phospho-PKM2 at either 2 or 6 h post-treatment. *B*, Western blotting showing proteins related with oncogenic signaling, GLS, GYS, GLUTs, HKII, PDHA1, and phospho-PDHA1. Total protein lysates were isolated from cells treated with gefitinib or erlotinib for 6 h. Equivalent amounts of proteins from whole-cell lysates were subjected to Western blot analysis to detect the indicated proteins. β-Actin was used as a loading control.

(Fig. 5*B*). Lactate dehydrogenase A (LDHA), p-LDHA, pyruvate dehydrogenase α1 (PDHA1), and p-PDHA1 were not altered in HCC827 and PC-9 cells after 6 h treatment with TKIs (Fig. 5*B*).

EGFR Signaling Pathway Down-regulates the Glucose Transporter GLUT3—GLUT1 (glucose transporter 1, *SLC2A1*) and GLUT3 (glucose transporter 3, *SLC2A3*) were mainly expressed in LAD cells (supplemental Table S2). Western blot analysis showed that GLUT3, but not GLUT1, was decreased in HCC827 and PC-9 cells after 6 h of treatment with TKIs. To further confirm membrane-bound GLUT3 expression levels, we investigated the effects of EGFR-TKIs on membrane-bound glucose transporters in HCC827, PC-9, and H1975 cells by flow cytometry. We observed reduction of membrane-bound GLUT3 in the EGFR TKI-sensitive cell lines HCC827 (Fig. 6, *A* and *B*) and PC-9 (Fig. 6, *C* and *D*), although the expression of GLUT3 was unchanged in TKI-resistant H1975 cells (Fig. 6, *E* and *F*) after 6 h of TKI treatment.

To gain additional insight into the functional role of glucose transport, we measured 3-O-(^{3}H-methyl)-D-glucose (3-OMeG) uptake in the absence or presence of EGFR-TKIs. Following 6-hr treatment with gefitinib or erlotinib, the 3-OMeG transport rate in HCC827 and PC-9 cells significantly decreased (Fig. 6, *G* and *H*).

Alterations in Additional Metabolic Pathways other than Glycolysis and PPP in the Response to Erlotinib Treatment—To further characterize whether EGFR signaling regulates additional metabolic pathways other than glycolysis and PPP, we quantified metabolites in tricarboxylic acid (TCA), amino acids, and redox. Despite equivalent amount of acetyl-CoA and citrate, fumarate (FA) and malate (MA) were decreased in HCC827 and PC-9 cells but not in H1975 cells after 6 h treatment with erlotinib (Fig. 7*A* and supplemental Table S1). This result suggests that glutaminolysis was down-regulated after inhibition of EGFR signaling, consistent with the lower expression levels of GLS (Fig. 5*B*). In contrast, amino acids such as proline (Pro) and aspartate (Asp) were increased in TKI-sensitive HCC827 and PC9 cells as compared with TKI-resistant H1975 cells (Fig. 7*A* and supplemental Table S1). Additionally, reductive nicotinamide adenine dinucleotide (NADH) and reductive glutathione (GSH) were significantly reduced in HCC827 and PC9 cells, while conversely oxidative glutathione (GSSG) was increased in H1975 cells (Fig. 7*A* and supplemental Table S1).

EGFR Signaling Is Required for de Novo Pyrimidine Biosynthesis—*N*-Carbamoyl-aspartate (NC-Asp) levels were decreased after EGFR-TKI treatment as determined by metabolome analysis (Fig. 7*A*). Consistent with this observation, the phosphorylation of ribosomal protein S6 kinase 1 (S6K) and carbamoyl-phosphate synthetase 2, aspartate transcarbamoylase, dihydroorotase (CAD) were obviously down-regulated in HCC827 and PC9 cells but not in H1975 cells (Fig. 7*B*). The phosphorylation of the Ser1859 residue in CAD protein is required for the first step in the *de novo* synthesis of pyrimidines (35). These data imply that the inhibition of EGFR signaling alters *de novo* pyrimidine biosynthesis in EGFR-mutated LAD cells.

DISCUSSION

In this report, we demonstrated that EGFR signaling up-regulated aerobic glycolysis in EGFR-mutated LAD cells. EGFR signaling regulates functional GLUT3 to control the glycolysis and pentose phosphate pathways. Moreover, EGFR signaling activated *de novo* pyrimidine synthesis, which is regulated by

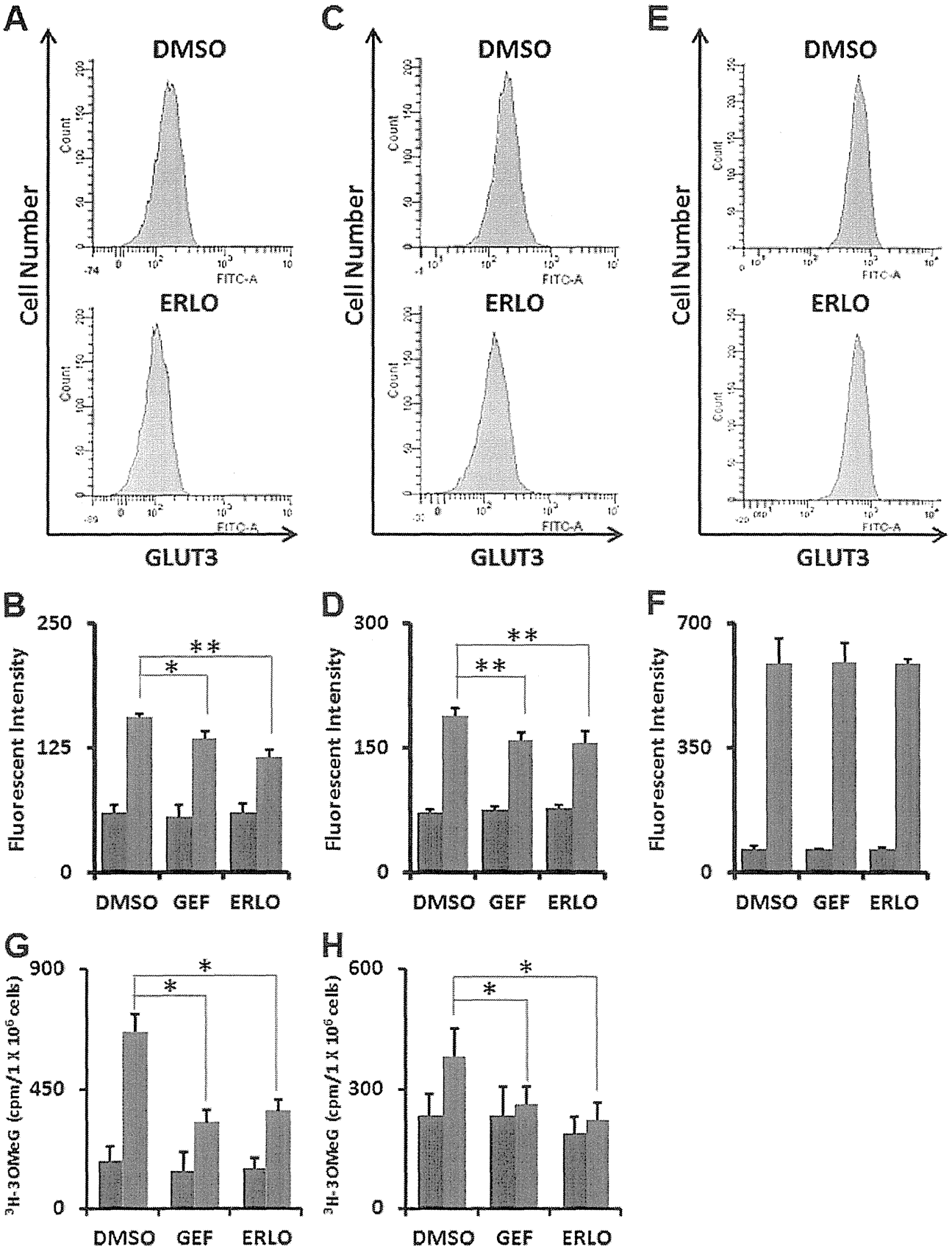

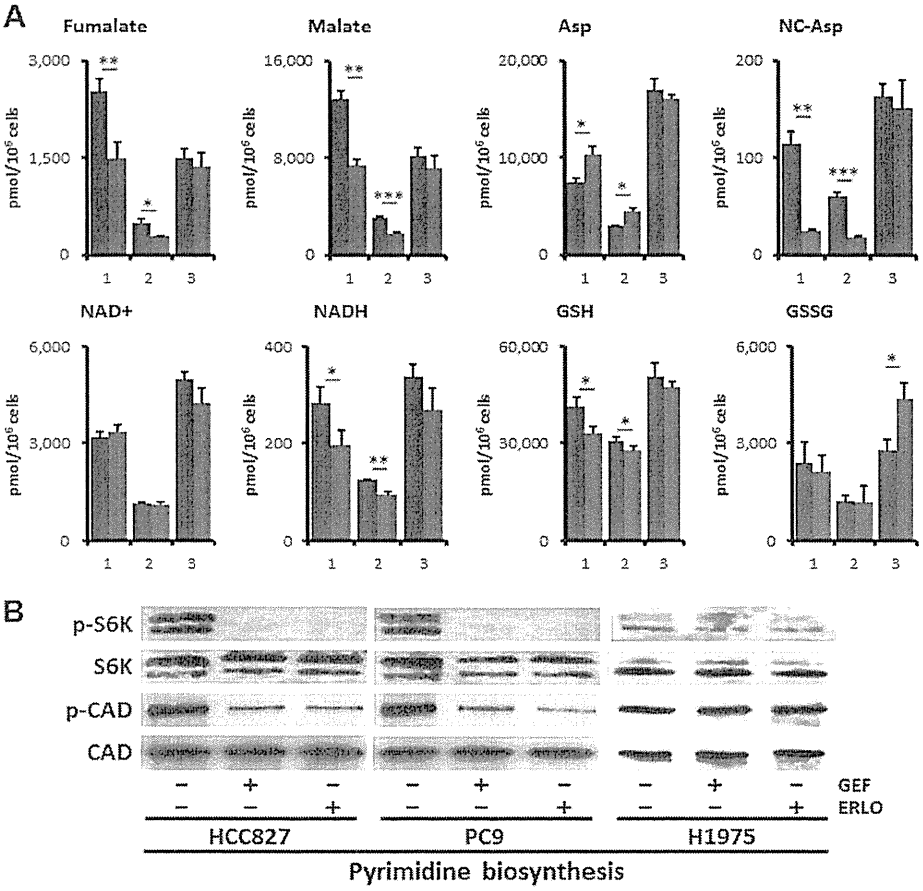

FIGURE 7. **EGFR signaling maintains *de novo* pyrimidine biosynthesis pathway.** *A*, metabolome analysis. Intracellular concentration (pmol/million cells) of key metabolites involved in glycolysis and pentose phosphate pathway (*PPP*) after inhibition of EGFR signaling is shown. Error bars indicate S.D. ($n = 3$). Total metabolites were extracted with methanol from HCC827, PC9, or H1975 cells treated with DMSO (*blue*) or erlotinib (*red*, 1 μM) for 6 h. Representative metabolites such as fumarate (*FA*), malate (*MA*), aspartate (*Asp*), *N*-carbamoyl-aspartate (NC-Asp), NAD^+, NADH, reductive glutathione (*GSH*), and oxidative glutathione (*GSSG*) are shown here. *B*, Western blot showing proteins related with *de novo* pyrimidine synthesis. Total protein lysates were isolated from cells treated with gefitinib (1 μM) or erlotinib (1 μM) for 6 h. Equivalent amounts of proteins from whole-cell lysates were subjected to Western blot analysis to detect the indicated proteins. Ribosomal protein S6 kinase 1 (S6K), phospho-S6K (p-S6K, Thr421/Ser424) and carbamoyl-phosphate synthetase 2, aspartate transcarbamoylase, dihydroorotase (CAD), and phospho-CAD (p-CAD, Ser-1859) are shown.

CAD activity. We conclude that EGFR signaling regulates global metabolic pathways in EGFR-mutated LAD cells. Our data provide evidence that may link the EGFR-TKI response to the regulation of metabolism in EGFR-mutated LAD. Inhibition of EGFR signaling abrogated the Warburg effect by inhibiting multiple steps including MYC-driven transcription and phosphorylation of PKM2 to regulate glycolysis in LAD. We comprehensively quantified the key metabolites in glycolysis and PPP and identified glucose transport as the most important regulatory step for controlling glucose metabolism in LAD cells during EGFR signaling. This observation is consistent with a previous study demonstrating that gefitinib treatment decreased glucose transport efficiency and hexokinase activity in TKI-sensitive LAD cells (26).

The molecular mechanism by which EGFR signaling regulates glucose transport is still unclear. Weihua *et al.* found that EGFR physically associated with and stabilized the sodium/glucose transporter (SGLT1) to promote glucose uptake into cancer

FIGURE 6. **Glucose transport efficiency is the most rapid and critically regulated function of glucose metabolism linked to EGFR signaling.** *A*, representative flow cytometry plot of GLUT3 expression in HCC827 cells treated with erlotinib (1 μM) or DMSO as a control for 6 h. After fixation, cells were stained with a rabbit anti-GLUT3 antibody and FITC-conjugated anti-rabbit secondary antibody. *B*, flow cytometric analysis of GLUT3 expression in HCC827 cells. *Blue bars* show background fluorescence with IgG isotype control while *red bars* indicate fluorescence staining results with anti-GLUT3 Ab. Error bars indicate S.D. ($n = 4$). *, $p < 0.05$; **, $p < 0.01$ *versus* control by two-tailed Student's *t* test. *C*, representative flow cytometry plot of GLUT3 expression in PC9 cells treated with erlotinib (1 μM) or DMSO as a control for 6 h. After fixation, cells were stained with a rabbit anti-GLUT3 antibody and FITC-conjugated anti-rabbit secondary antibody. *D*, flow cytometric analysis of GLUT1 expression in PC9 cells. *Blue bars* show background fluorescence with IgG isotype control while *red bars* indicate fluorescence staining results with anti-GLUT3 Ab. Error bars indicate S.D. ($n = 4$). *, $p < 0.05$; **, $p < 0.01$ *versus* control by two-tailed Student's *t* test. *E*, representative flow cytometry plot of GLUT3 expression in TKI-resistant H1975 cells treated with erlotinib (1 μM) or DMSO as a control for 6 h. After fixation, cells were stained with a rabbit anti-GLUT3 antibody and FITC-conjugated anti-rabbit secondary antibody. *F*, flow cytometric analysis of GLUT3 expression in TKI-resistant H1975 cells. *Blue bars* show background fluorescence with IgG isotype control while *red bars* indicate fluorescence staining results with anti-GLUT3 Ab. Error bars indicate S.D. ($n = 4$). *, $p < 0.05$; **, $p < 0.01$ *versus* control by two-tailed Student's *t* test. *G* and *H*, 3-*O*-([^{3}H]methyl)-D-glucose (3-OMeG) transport efficiency in HCC827 (*G*) and PC-9 (*H*) cells in response to gefitinib or erlotinib as compared with DMSO control. Cells were treated with indicated TKIs (1 μM) for 6 h before transport assay. Radioactivity was measured over time. Cells were harvested at 1 min (*blue*) and 10 min (*red*) after addition of 3-OMeG. Error bars indicate S.D. ($n = 4$). *, $p < 0.001$ *versus* control by two-tailed Student's *t* test.

cells (36). However, this function did not require EGFR kinase activity. In this report, we found that TKIs to EGFR, gefitinib, and erlotinib, repressed aerobic glycolysis and PPP in EGFR-mutated LAD cells. Although SGLT1 directly interacts with EGFR, EGFR signaling may regulate GLUT translocation in an indirect manner. Mutated EGFRs found in LAD have constitutive tyrosine kinase activity, resulting in activation of downstream RAS/MAPK and PI3K/AKT pathways (Figs. 4*A* and 5*B*). In adipocytes and skeletal muscle, insulin and the PI3K/AKT pathway mediate GLUT4 translocation (37, 38). To promote glucose uptake into muscle and fat cells, insulin stimulates the translocation of GLUT4 from intracellular membranes to the cell surface. Insulin signals go through AS160 (Akt substrate of 160 kDa) and Tbc1Ds to modulate Rab GTPase, and through Rho GTPase TC10a to act on other targets (37, 38). The EGFR-PI3K/AKT axis might control GLUT translocation to the plasma membrane in EGFR-mutated LAD cells. To prove this, we would need to characterize in more detail the molecular mechanisms that control GLUT expression, activity, and translocation.

A recent study showed that AMPK-dependent degradation of thioredoxin-interacting protein (TXNIP) upon stress led to enhanced glucose uptake via GLUT1 (39). Another research report showed that tumor-associated mutant p53 (mutp53) stimulated the Warburg effect in cancer cells as a new mutp53 gain of function (40). Mutp53 did not affect the expression of GLUT1, but promoted aerobic glycolysis by inducing GLUT1 translocation to the plasma membrane, which was mediated by activated RHOA and its downstream effector ROCK. In this study, the EGFR-TKI-sensitive LAD cell lines HCC827 and PC9 possess mutp53, but not the H1975 cell line. A possible molecular mechanism is that either EGFR signaling may regulate GLUT translocation by directly activating the RHOA/ROCK pathway or the mutp53 pathway that in turn activates RHOA/ROCK function. Further experiments would be required to determine whether EGFR signaling controls glucose transport through the TXNIP or mutp53 pathway.

New therapeutic strategies are currently needed to overcome the EGFR T790M-mediated acquired resistance observed in the clinic (8). A recent Phase III study of afatinib monotherapy failed to show overall survival benefit in patients with acquired resistance to reversible EGFR-TKIs(41). Kim *et al.* showed that targeting of glycolysis was an effective therapeutic option to overcome the limited efficacy of afatinib in LAD cells with EGFR T790M (42). Treatment with 2DG completely shut down lactate production in EGFR-mutated LAD cells (Fig. 2*B*), since 2DG is a glucose analog that competes with glucose for cellular uptake. Therefore, combination therapies of EGFR-TKIs and drugs that block the glycolysis pathway such as GLUT-inhibitors would be expected to be much more effective for TKI-resistant cases.

Molecular targeting therapy using TKIs is currently one of the most successful forms of treatment in the clinic, and includes imatinib targeting BCR-ABL in chronic myeloid leukemia (CML) and gefitinib/erlotinib in EGFR-mutated LAD (3). Despite high therapeutic responses to EGFR-TKI treatment, it is clear that not all patients experience benefit; thus, there is still a need to identify potential non-responders and match patients with the most effective therapies (4). Monitoring of tumor glucose utilization by [^{18}F]fluorodeoxyglucose (FDG)-positron emission tomography (PET) was implemented for the early prediction of treatment response to EGFR-TKIs in NSCLC (26, 43). In this report, we demonstrate that TKIs to EGFR, gefitinib and erlotinib, repress aerobic glycolysis in EGFR-mutated LAD cells. Those correlations strongly suggest that intermediate metabolites in the pentose phosphate pathway, glycolysis, and pyrimidine biosynthesis such as FBP, DHAP, LA, 6PG, and NC-Asp could serve as well-defined biomarkers to predict response to EGFR-TKI therapy.

The application of metabolomics in oncology has focused its ability to identify biomarkers for cancer diagnosis, prognosis, and therapeutic efficacy (44). In our previous study, we compared the metabolomics of normal and tumor tissues surgically resected pairwise from nine lung patients using CE-TOFMS to elucidate tumor-specific metabolism (45). Significantly high lactate concentrations and elevated activating phosphorylation levels of phosphofructokinase and pyruvate kinase in lung tumors confirmed hyperactive glycolysis (45). Here we show that EGFR signaling regulates many metabolites in EGFR-mutated LAD cells under *in vitro* culture conditions; however, whether EGFR-TKIs have the same effects *in vivo* is still unknown. To build upon this work, further investigations will explore these concepts in relevant animal models and in LAD tissue biopsy samples using bronchoscope before and after EGFR-TKI therapy. *In vivo* validation of these concepts will have significant implications for future diagnostic and therapeutic possibilities for patients.

Acknowledgments—We thank all of Dr. Tsuchihara's laboratory members for help. We also thank Dr. Phillip Wong for carefully reading the manuscript and providing critical comments.

REFERENCES

1. da Cunha Santos, G., Shepherd, F. A., and Tsao, M. S. (2011) EGFR mutations and lung cancer. *Annu. Rev. Pathol.* **6,** 49–69
2. Irmer, D., Funk, J. O., and Blaukat, A. (2007) EGFR kinase domain mutations - functional impact and relevance for lung cancer therapy. *Oncogene* **26,** 5693–5701
3. Levitzki, A. (2013) Tyrosine kinase inhibitors: views of selectivity, sensitivity, and clinical performance. *Annu. Rev. Pharmacol. Toxicol.* **53,** 161–185
4. Linardou, H., Dahabreh, I. J., Bafaloukos, D., Kosmidis, P., and Murray, S. (2009) Somatic EGFR mutations and efficacy of tyrosine kinase inhibitors in NSCLC. *Nat. Rev. Clin. Oncol.* **6,** 352–366
5. Suzuki, A., Mimaki, S., Yamane, Y., Kawase, A., Matsushima, K., Suzuki, M., Goto, K., Sugano, S., Esumi, H., Suzuki, Y., and Tsuchihara, K. (2013) Identification and characterization of cancer mutations in Japanese lung adenocarcinoma without sequencing of normal tissue counterparts. *PLoS One* **8,** e73484
6. Imielinski, M., Berger, A. H., Hammerman, P. S., Hernandez, B., Pugh, T. J., Hodis, E., Cho, J., Suh, J., Capelletti, M., Sivachenko, A., Sougnez, C., Auclair, D., Lawrence, M. S., Stojanov, P., Cibulskis, K., Choi, K., de Waal, L., Sharifnia, T., Brooks, A., Greulich, H., Banerji, S., Zander, T., Seidel, D., Leenders, F., Ansén, S., Ludwig, C., Engel-Riedel, W., Stoelben, E., Wolf, J., Goparju, C., Thompson, K., Winckler, W., Kwiatkowski, D., Johnson, B. E., Jänne, P. A., Miller, V. A., Pao, W., Travis, W. D., Pass, H. I., Gabriel, S. B., Lander, E. S., Thomas, R. K., Garraway, L. A., Getz, G., and Meyerson, M. (2012) Mapping the Hallmarks of Lung Adenocarcinoma with Massively Parallel Sequencing. *Cell* **150,** 1107–1120
7. Mellinghoff, I. (2007) Why do cancer cells become "addicted" to oncogenic epidermal growth factor receptor? *Plos Med.* **4,** 1620–1622

8. Pao, W., and Chmielecki, J. (2010) Rational, biologically based treatment of EGFR-mutant non-small-cell lung cancer. *Nature Reviews Cancer* **10,** 760–774
9. Lemmon, M. A., and Schlessinger, J. (2010) Cell signaling by receptor tyrosine kinases. *Cell* **141,** 1117–1134
10. Cairns, R. A., Harris, I. S., and Mak, T. W. (2011) Regulation of cancer cell metabolism. *Nat. Rev. Cancer* **11,** 85–95
11. Levine, A. J., and Puzio-Kuter, A. M. (2010) The control of the metabolic switch in cancers by oncogenes and tumor suppressor genes. *Science* **330,** 1340–1344
12. Cheong, H., Lu, C., Lindsten, T., and Thompson, C. B. (2012) Therapeutic targets in cancer cell metabolism and autophagy. *Nat. Biotechnol.* **30,** 671–678
13. Ying, H., Kimmelman, A. C., Lyssiotis, C. A., Hua, S., Chu, G. C., Fletcher-Sananikone, E., Locasale, J. W., Son, J., Zhang, H., Coloff, J. L., Yan, H., Wang, W., Chen, S., Viale, A., Zheng, H., Paik, J. H., Lim, C., Guimaraes, A. R., Martin, E. S., Chang, J., Hezel, A. F., Perry, S. R., Hu, J., Gan, B., Xiao, Y., Asara, J. M., Weissleder, R., Wang, Y. A., Chin, L., Cantley, L. C., and DePinho, R. A. (2012) Oncogenic Kras maintains pancreatic tumors through regulation of anabolic glucose metabolism. *Cell* **149,** 656–670
14. Lunt, S. Y., and Vander Heiden, M. G. (2011) Aerobic glycolysis: meeting the metabolic requirements of cell proliferation. *Annu. Rev. Cell Dev. Biol.* **27,** 441–464
15. Soga, T. (2013) Cancer metabolism: key players in metabolic reprogramming. *Cancer Sci.* **104,** 275–281
16. Vander Heiden, M. G., Cantley, L. C., and Thompson, C. B. (2009) Understanding the Warburg effect: the metabolic requirements of cell proliferation. *Science* **324,** 1029–1033
17. Hitosugi, T., Kang, S., Vander Heiden, M. G., Chung, T. W., Elf, S., Lythgoe, K., Dong, S., Lonial, S., Wang, X., Chen, G. Z., Xie, J., Gu, T. L., Polakiewicz, R. D., Roesel, J. L., Boggon, T. J., Khuri, F. R., Gilliland, D. G., Cantley, L. C., Kaufman, J., and Chen, J. (2009) Tyrosine phosphorylation inhibits PKM2 to promote the Warburg effect and tumor growth. *Sci. Signal* **2,** ra73
18. Hitosugi, T., and Chen, J. (2013) Post-translational modifications and the Warburg effect. *Oncogene* doi:10.1038/onc.2013.406
19. Miller, D. M., Thomas, S. D., Islam, A., Muench, D., and Sedoris, K. (2012) c-Myc and cancer metabolism. *Clin. Cancer Res.* **18,** 5546–5553
20. Yang, W., and Lu, Z. (2013) Nuclear PKM2 regulates the Warburg effect. *Cell Cycle* **12,** 3154–3158
21. Wong, N., Ojo, D., Yan, J., and Tang, D. (2014) PKM2 contributes to cancer metabolism. *Cancer Lett.* doi: 10.1016/j.canlet. 2014.01.031
22. Babic, I., Anderson, E. S., Tanaka, K., Guo, D., Masui, K., Li, B., Zhu, S., Gu, Y., Villa, G. R., Akhavan, D., Nathanson, D., Gini, B., Mareninov, S., Li, R., Camacho, C. E., Kurdistani, S. K., Eskin, A., Nelson, S. F., Yong, W. H., Cavenee, W. K., Cloughesy, T. F., Christofk, H. R., Black, D. L., and Mischel, P. S. (2013) EGFR mutation-induced alternative splicing of Max contributes to growth of glycolytic tumors in brain cancer. *Cell Metab.* **17,** 1000–1008
23. Soga, T., and Heiger, D. N. (2000) Amino acid analysis by capillary electrophoresis electrospray ionization mass spectrometry. *Anal. Chem.* **72,** 1236–1241
24. Soga, T., Ueno, Y., Naraoka, H., Ohashi, Y., Tomita, M., and Nishioka, T. (2002) Simultaneous determination of anionic intermediates for Bacillus subtilis metabolic pathways by capillary electrophoresis electrospray ionization mass spectrometry. *Anal. Chem.* **74,** 2233–2239
25. Soga, T., Ohashi, Y., Ueno, Y., Naraoka, H., Tomita, M., and Nishioka, T. (2003) Quantitative metabolome analysis using capillary electrophoresis mass spectrometry. *J. Proteome Res.* **2,** 488–494
26. Su, H., Bodenstein, C., Dumont, R. A., Seimbille, Y., Dubinett, S., Phelps, M. E., Herschman, H., Czernin, J., and Weber, W. (2006) Monitoring tumor glucose utilization by positron emission tomography for the prediction of treatment response to epidermal growth factor receptor kinase inhibitors. *Clin. Cancer Res.* **12,** 5659–5667
27. Okamoto, K., Okamoto, I., Okamoto, W., Tanaka, K., Takezawa, K., Kuwata, K., Yamaguchi, H., Nishio, K., and Nakagawa, K. (2010) Role of survivin in EGFR inhibitor-induced apoptosis in non-small cell lung cancers positive for EGFR mutations. *Cancer Res.* **70,** 10402–10410
28. Donev, I. S., Wang, W., Yamada, T., Li, Q., Takeuchi, S., Matsumoto, K., Yamori, T., Nishioka, Y., Sone, S., and Yano, S. (2011) Transient PI3K inhibition induces apoptosis and overcomes HGF-mediated resistance to EGFR-TKIs in EGFR mutant lung cancer. *Clin. Cancer Res.* **17,** 2260–2269
29. Zhou, W., Ercan, D., Chen, L., Yun, C. H., Li, D., Capelletti, M., Cortot, A. B., Chirieac, L., Iacob, R. E., Padera, R., Engen, J. R., Wong, K. K., Eck, M. J., Gray, N. S., and Jänne, P. A. (2009) Novel mutant-selective EGFR kinase inhibitors against EGFR T790M. *Nature* **462,** 1070–1074
30. Sudo, M., Chin, T. M., Mori, S., Doan, N. B., Said, J. W., Akashi, M., and Koeffler, H. P. (2013) Inhibiting proliferation of gefitinib-resistant, non-small cell lung cancer. *Cancer Chemother. Pharmacol.* **71,** 1325–1334
31. Sonveaux, P., Végran, F., Schroeder, T., Wergin, M. C., Verrax, J., Rabbani, Z. N., De Saedeleer, C. J., Kennedy, K. M., Diepart, C., Jordan, B. F., Kelley, M. J., Gallez, B., Wahl, M. L., Feron, O., and Dewhirst, M. W. (2008) Targeting lactate-fueled respiration selectively kills hypoxic tumor cells in mice. *J. Clin. Invest.* **118,** 3930–3942
32. Morrish, F., Neretti, N., Sedivy, J. M., and Hockenbery, D. M. (2008) The oncogene c-Myc coordinates regulation of metabolic networks to enable rapid cell cycle entry. *Cell Cycle* **7,** 1054–1066
33. Osthus, R. C., Shim, H., Kim, S., Li, Q., Reddy, R., Mukherjee, M., Xu, Y., Wonsey, D., Lee, L. A., and Dang, C. V. (2000) Deregulation of glucose transporter 1 and glycolytic gene expression by c-Myc. *J. Biol. Chem.* **275,** 21797–21800
34. David, C. J., Chen, M., Assanah, M., Canoll, P., and Manley, J. L. (2010) HnRNP proteins controlled by c-Myc deregulate pyruvate kinase mRNA splicing in cancer. *Nature* **463,** 364–368
35. Ben-Sahra, I., Howell, J. J., Asara, J. M., and Manning, B. D. (2013) Stimulation of de novo pyrimidine synthesis by growth signaling through mTOR and S6K1. *Science* **339,** 1323–1328
36. Weihua, Z., Tsan, R., Huang, W. C., Wu, Q., Chiu, C. H., Fidler, I. J., and Hung, M. C. (2008) Survival of cancer cells is maintained by EGFR independent of its kinase activity. *Cancer Cell* **13,** 385–393
37. Watson, R. T., and Pessin, J. E. (2006) Bridging the GAP between insulin signaling and GLUT4 translocation. *Trends Biochem. Sci.* **31,** 215–222
38. Bogan, J. S. (2012) Regulation of glucose transporter translocation in health and diabetes. *Annu. Rev. Biochem.* **81,** 507–532
39. Wu, N., Zheng, B., Shaywitz, A., Dagon, Y., Tower, C., Bellinger, G., Shen, C. H., Wen, J., Asara, J., McGraw, T. E., Kahn, B. B., and Cantley, L. C. (2013) AMPK-dependent degradation of TXNIP upon energy stress leads to enhanced glucose uptake via GLUT1. *Mol. Cell* **49,** 1167–1175
40. Zhang, C., Liu, J., Liang, Y., Wu, R., Zhao, Y., Hong, X., Lin, M., Yu, H., Liu, L., Levine, A. J., Hu, W., and Feng, Z. (2013) Tumour-associated mutant p53 drives the Warburg effect. *Nat. Commun.* **4,** 2935
41. Miller, V. A., Hirsh, V., Cadranel, J., Chen, Y. M., Park, K., Kim, S. W., Zhou, C., Su, W. C., Wang, M., Sun, Y., Heo, D. S., Crino, L., Tan, E. H., Chao, T. Y., Shahidi, M., Cong, X. J., Lorence, R. M., and Yang, J. C. (2012) Afatinib versus placebo for patients with advanced, metastatic non-small-cell lung cancer after failure of erlotinib, gefitinib, or both, and one or two lines of chemotherapy (LUX-Lung 1): a phase 2b/3 randomised trial. *Lancet Oncol.* **13,** 528–538
42. Kim, S. M., Yun, M. R., Hong, Y. K., Solca, F., Kim, J. H., Kim, H. J., and Cho, B. C. (2013) Glycolysis inhibition sensitizes non-small cell lung cancer with T790M mutation to irreversible EGFR inhibitors via translational suppression of Mcl-1 by AMPK activation. *Mol. Cancer Ther.* **12,** 2145–2156
43. Takahashi, R., Hirata, H., Tachibana, I., Shimosegawa, E., Inoue, A., Nagatomo, I., Takeda, Y., Kida, H., Goya, S., Kijima, T., Yoshida, M., Kumagai, T., Kumanogoh, A., Okumura, M., Hatazawa, J., and Kawase, I. (2012) Early [18F]fluorodeoxyglucose positron emission tomography at two days of gefitinib treatment predicts clinical outcome in patients with adenocarcinoma of the lung. *Clin. Cancer Res.* **18,** 220–228
44. Spratlin, J. L., Serkova, N. J., and Eckhardt, S. G. (2009) Clinical applications of metabolomics in oncology: a review. *Clin. Cancer Res.* **15,** 431–440
45. Kami, K., Fujimori, T., Sato, H., Sato, M., Yamamoto, H., Ohashi, Y., Sugiyama, N., Ishihama, Y., Onozuka, H., Ochiai, A., Esumi, H., Soga, T., and Tomita, M. (2013) Metabolomic profiling of lung and prostate tumor tissues by capillary electrophoresis time-of-flight mass spectrometry. *Metabolomics* **9,** 444–453

Metabolism:

Epidermal Growth Factor Receptor (EGFR) Signaling Regulates Global Metabolic Pathways in EGFR-mutated Lung Adenocarcinoma

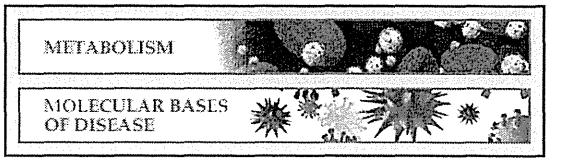

Hideki Makinoshima, Masahiro Takita, Shingo Matsumoto, Atsushi Yagishita, Satoshi Owada, Hiroyasu Esumi and Katsuya Tsuchihara

J. Biol. Chem. 2014, 289:20813-20823.
doi: 10.1074/jbc.M114.575464 originally published online June 13, 2014

Cancer Science
Japanese Cancer Association JCA
Open Access

Phase II study of FOLFIRINOX for chemotherapy-naïve Japanese patients with metastatic pancreatic cancer

Takuji Okusaka,[1] Masafumi Ikeda,[2] Akira Fukutomi,[3] Tatsuya Ioka,[4] Junji Furuse,[5] Shinichi Ohkawa,[6] Hiroyuki Isayama[7] and Narikazu Boku[8]

[1]Department of Hepatobiliary and Pancreatic Oncology, National Cancer Center Hospital, Tokyo; [2]Department of Hepatobiliary and Pancreatic Oncology, National Cancer Center Hospital East, Kashiwa; [3]Department of Gastrointestinal Oncology, Sunto-gun Cancer Center, Shizuoka; [4]Department of Hepatobiliary and Pancreatic Oncology, Osaka Medical Center for Cancer and Cardiovascular Diseases, Osaka; [5]Department of Medical Oncology, Kyorin University School of Medicine, Mitaka; [6]Department of Hepatobiliary and Pancreatic Oncology, Kanagawa Cancer Center, Yokohama; [7]Department of Gastroenterology, Graduate School of Medicine, The University of Tokyo, Tokyo; [8]Department of Clinical Oncology, St. Marianna University School of Medicine, Kawasaki, Japan

Key words
Chemotherapy, FOLFIRINOX, irinotecan, oxaliplatin, pancreatic cancer

Correspondence
Takuji Okusaka, Department of Hepatobiliary and Pancreatic Oncology, National Cancer Center Hospital, Tsukiji 5-1-1, Chuo-ku, Tokyo 104-0045, Japan.
Tel.: +81-3-3542-2511; Fax: +81-3-3542-3815;
E-mail: tokusaka@ncc.go.jp

Funding Information
Yakult Honsha Co., Ltd.

Received May 8, 2014; Revised July 24, 2014; Accepted August 5, 2014

Cancer Sci **105** (2014) 1321–1326

doi: 10.1111/cas.12501

The FOLFIRINOX combination of chemotherapy drugs had not been fully evaluated for Japanese pancreatic cancer patients. Therefore, we carried out a phase II study to examine the efficacy and safety of FOLFIRINOX in chemotherapy-naïve Japanese patients with metastatic pancreatic cancer. FOLFIRINOX (i.v. infusion of 85 mg/m^2 oxaliplatin, 180 mg/m^2 irinotecan, and 200 mg/m^2 *l*-leucovorin, followed by a bolus of 400 mg/m^2 fluorouracil and a 46-h continuous infusion of 2400 mg/m^2 fluorouracil) was given every 2 weeks. The primary endpoint was the response rate. The 36 enrolled patients received a median of eight (range, 1–25) treatment cycles. The response rate was 38.9% (95% confidence interval [CI], 23.1–56.5); median overall survival, 10.7 months (95% CI, 6.9–13.2); and median progression-free survival, 5.6 months (95% CI, 3.0–7.8). Major grade 3 or 4 toxicities included neutropenia (77.8%), febrile neutropenia (22.2%), thrombocytopenia (11.1%), anemia (11.1%), anorexia (11.1%), diarrhea (8.3%), nausea (8.3%), elevated alanine aminotransferase levels (8.3%), and peripheral sensory neuropathy (5.6%). Febrile neutropenia occurred only during the first cycle. There were no treatment-related deaths. FOLFIRINOX can be a standard regimen showing favorable efficacy and acceptable toxicity profile in chemotherapy-naïve Japanese patients with metastatic pancreatic cancer.

Pancreatic cancer is the eighth leading cause of cancer-related deaths worldwide, with approximately 266 000 deaths reported in 2008.[1] In Japan, approximately 30 000 people die of pancreatic cancer annually, accounting for 8.3% of all malignant neoplasm-related deaths.[2] Pancreatic cancer is associated with an extremely poor prognosis, with the reported 5-year survival rates in male and female patients being only 7.1% and 6.9%, respectively, in Japan.[3]

In a randomized study, GEM monotherapy showed significant improvements in OS and clinical benefit response compared to 5-FU.[4] Thereafter, it has been recognized as the standard regimen for pancreatic cancer. Various GEM-based combination regimens have been investigated, without any evidence of additional survival benefits. The only exception is erlotinib, which, when combined with GEM, has been shown to provide a statistically significant improvement in OS,[5] although the absolute difference at median survival time was only marginal (0.3 months). Gemcitabine monotherapy has remained the standard therapy. Accordingly, more effective treatment options are urgently needed.

In a phase II/III study in 2011, Conroy *et al.*[6] showed a significant improvement in OS and quality of life with FOLFIRINOX (oxaliplatin, irinotecan, 5-FU, and leucovorin) compared to GEM in patients with MPC. Since then, FOLFIRINOX has become the standard treatment for patients with pancreatic cancer with a good PS in North America and Europe. However, the safety and efficacy of this regimen in Japanese patients has not been evaluated. Accordingly, we carried out a phase II study of FOLFIRINOX in Japanese patients with MPC.

Materials and Methods

Patients. The inclusion criteria were: histologically or cytologically confirmed pancreatic adenocarcinoma or adenosquamous carcinoma; an Eastern Cooperative Oncology Group PS of 0 or 1; age 20–75 years; MPC with at least one measurable lesion; and adequate hematological, liver, and renal function (hemoglobin ≥9.0 g/dL, white blood cell count ≤10 000/mm^3, neutrophil count ≥2000/mm^3, platelet count ≥100 000/mm^3, total bilirubin ≤ upper limit of normal, aspartate transaminase and alanine transaminase ≤2.5× upper limit of normal, creatinine ≤1.2 mg/dL, and C-reactive protein ≤2.0 mg/dL).

Patients were excluded if they had: received prior chemotherapy or radiation therapy; grade 2 or higher peripheral sensory neuropathy; blood transfusion, blood products, or hematopoietic growth factor preparations such as G-CSF within 7 days before enrolment; UGT genetic polymorphisms of homozygous *UGT1A1*28* or *UGT1A1*6* or heterozygous *UGT1A1*6* and *UGT1A1*28*; apparent coelomic fluid (pleural effusion, ascites, or pericardial fluid) or peritoneal

dissemination; diarrhea including watery stools within 3 days before enrolment; poorly controlled diabetes; synchronous or metachronous double cancer, excluding carcinoma *in situ* or intramucosal carcinoma cured by local treatment; active infection; or other serious concomitant diseases.

The study was carried out in accordance with the Declaration of Helsinki and the Good Clinical Practice guidelines. The protocol was approved by the ethics committees of all participating institutions, and informed consent was obtained from all patients before their enrolment in the study.

Study design. This study was an open-label, multicenter, single-arm phase II study. To ensure the safety of the patients, the study consisted of two stages. In the first stage, the IDMC evaluated the feasibility of the regimen during the initial two cycles in the first 10 patients to determine proceeding to the next stage or not. For careful safety evaluation, the first 10 patients were required to be hospitalized until the end of the third cycle of treatment. If more than half of the patients withdrew from the study treatment because of toxicities by the completion of the second cycle or if the IDMC decided that the study had to be discontinued, the trial would be terminated. If feasibility was confirmed in the first stage, an additional 25 patients would be enrolled in the second stage. The decision as to whether these additional patients would be treated as inpatients or outpatients was made by the investigators. The final analysis would be carried out 12 months after enrolment of the last patient.

The primary endpoint was the RR, and the secondary endpoints were OS PFS, and safety for all of the patients including those in the first stage.

Treatment. Treatment with FOLFIRINOX was given as follows: 2-h i.v. infusion of oxaliplatin at 85 mg/m^2 and 2-h i.v. infusion of *l*-leucovorin at 200 mg/m^2 (during which irinotecan was also i.v. infused over 90 min at 180 mg/m^2), followed by an i.v. bolus of 5-FU at 400 mg/m^2 and continuous i.v. infusion of 5-FU over 46 h at 2400 mg/m^2. This regimen was repeated every 2 weeks. Prior to the study treatment, a 5-HT$_3$ receptor antagonist and dexamethasone were given. Selective neurokinin 1 receptor antagonistic antiemetics were recommended to alleviate nausea and vomiting; G-CSF was not allowed as primary prophylaxis. The treatment was continued until disease progression, unacceptable toxicity, discontinuation as decided by the investigators, or patient refusal.

Chemotherapy was delayed until recovery from the following criteria: neutrophil count <1500/mm^3, platelet count <75 000/mm^3, total bilirubin >1.5 mg/dL, grade 3 or higher peripheral sensory neuropathy, grade 2 or higher diarrhea, and watery stools.

When the predefined toxic events in the protocol occurred, dose adjustment was required. The reduced dose were set at 150 mg/m^2 and 120 mg/m^2 for irinotecan, 65 mg/m^2 and 50 mg/m^2 for oxaliplatin, and 1800 mg/m^2 and 1200 mg/m^2 for infusional 5-FU (for more detail, see Tables S1–S3).

Assessment. Complete blood counts, blood chemical tests, and physical examinations were carried out at least once a week until the end of the fifth cycle and every 2 weeks thereafter. In cases of grade 4 hematological toxicity, re-examination within 4 days was required. Computed tomography was carried out at least every 6 weeks. Tumor response was independently reviewed extramurally in accordance with Response Evaluation Criteria in Solid Tumors version 1.0. Safety was evaluated in accordance with the Common Terminology Criteria for Adverse Events version 4.0.

Statistical analysis. Patients who received the study drugs at least once and did not considerably violate the Good Clinical Practice guidelines were included in the safety analysis population. Of these patients, those who met the eligibility criteria were included in the FAS. Efficacy was analyzed in the FAS population.

The expected and threshold RRs for the FOLFIRINOX regimen were set as 30% and 10%, respectively, on the basis of the RRs associated with GEM and FOLFIRINOX (9.4% and 31.6%, respectively) in the phase II/III study of FOLFIRINOX by Conroy *et al.*[6] If an exact binomial test was carried out at a one-sided significance level of 2.5%, according to the binomial distribution for the null hypothesis that the threshold RR was 10%, a sample size of 29 subjects would result in a power of 81.2%. Accordingly, the target sample size was set at 35 subjects, to account for exclusion of patients from the FAS. The median survival time and corresponding 95% CIs for OS and PFS were estimated using the Kaplan–Meier method. Progression-free survival was defined as the time from Day 1 of Cycle 1 until the first event (progressive disease or death due to any cause). If no such event occurred in a patient, data for that patient were censored on the day of the last imaging procedure. Overall survival was defined as the time from Day 1 of Cycle 1 until death due to any cause. In the absence of an event, data were censored on the last day of survival confirmation.

Results

Patient characteristics. Between June 2011 and September 2012, 36 patients were enrolled from seven institutions. In January 2012, the IDMC evaluated the safety data of the first 10 patients who underwent two cycles of treatment and determined that the study could be continued. The patient characteristics at baseline are shown in Table 1. The median age was 61.5 years (range, 27–71), 58.3% of the patients had a PS 0, the primary site of the tumor was the head of the pancreas in 19.4% of patients, 16.7% of patients had a biliary stent, and 2.8% of patients experienced recurrence after resection. The major sites of metastasis were the liver and lymph nodes.

All 36 patients received the study drugs and met the eligibility criteria; thus, all 36 patients were included in both the safety analysis and the FAS.

Treatment exposure. The median number of treatment cycles was eight (range, 1–25). The median relative dose intensities of oxaliplatin, irinotecan, bolus 5-FU, infusional 5-FU, and *l*-leucovorin were 71.0%, 69.6%, 15.9%, 80.3%, and 82.7%, respectively (Table 2). Dose reduction and treatment delay occurred in 32 patients (88.9%). Neutropenia was the most frequent cause for both dose reduction and treatment delay (75.0% and 75.0%, respectively). The major reasons for discontinuation of the treatment were disease progression (75.0%) and adverse event (19.4%).

Efficacy. Partial response, SD, and progressive disease were observed in 14, 11, and 10 patients, respectively, and 1 patient was not evaluated because the patient came off the study before SD confirmation. The RR was 38.9% (95% CI, 23.1–56.5), and the disease control rate was 69.4% (95% CI, 51.9–83.7; Table 3). The median time to partial response was 49 days (range, 35–129), and the median duration of response was 170 days (range, 156–196).

The median follow-up time was 12.6 months. The median OS was 10.7 months (95% CI, 6.9–13.2; Fig. 1), and the median PFS was 5.6 months (95% CI, 3.0–7.8; Fig. 2). The 6-month and 1-year survival probabilities were 72.2% (95% CI, 54.5–84.0) and 41.5% (95% CI, 25.4–56.8), respectively.

Table 1. Characteristics of chemotherapy-naïve Japanese patients with metastatic pancreatic cancer treated with FOLFIRINOX (n = 36)

	n	%
Sex		
Male	24	66.7
Female	12	33.3
Age, years		
Median	61.5	
Range	27–71	
<65	29	80.6
≥65	7	19.4
ECOG performance status		
0	21	58.3
1	15	41.7
Body surface area (m^2)		
Median	1.68	
Range	1.32–1.96	
Type of tumor		
Adenocarcinoma	33	91.7
Adenosquamous carcinoma	3	8.3
Primary tumor location		
Head	7	19.4
Others	28	77.8
None (recurrence)	1	2.8
Metastatic sites		
Liver	31	86.1
Lymph node	20	55.6
Spleen	1	2.8
Stent or drainage		
No	30	83.3
Yes	6	16.7
*UGT1A1(*6/*28)*		
Wild/wild	25	69.4
Wild/heterozygous	6	16.7
Heterozygous/wild	5	13.9

ECOG, Eastern Cooperative Oncology Group; *UGT1A1*, uridine diphosphate-glucuronosyltransferase 1A1.

Table 2. Drug delivery in chemotherapy-naïve Japanese patients with metastatic pancreatic cancer treated with FOLFIRINOX (n = 36)

	Values	Range
Total no. of cycles	325	
Median cycle of treatment	8	1–25

Median relative dose-intensity per patient	%	Range
Oxaliplatin	70.98	24.1–100.0
Irinotecan	69.62	17.4–100.0
Fluorouracil bolus	15.86	4.40–100.0
Continuous fluorouracil	80.33	49.6–100.0
l-Leucovorin	82.71	62.2–100.0

Dose reductions	Per patient		Per cycle	
	n	%	n	%
Total	32	88.9	88	27.1
Main reason for reduction				
Neutropenia	27	75.0	77	23.7
Febrile neutropenia	5	13.9	5	1.5
Thrombocytopenia	6	16.7	7	2.2
Diarrhea with fever (≥38°C)	3	8.3	3	0.9
Mucositis (≥Grade 3)	1	2.8	1	0.3
Anaphylaxis	1	2.8	1	0.3
Peripheral sensory neuropathy	2	5.6	3	0.9
Investigator decision	7	19.4	8	2.5

Delayed cycles	Per patient		Per cycle†	
	n	%	n	%
Total	32	88.9	115	39.8
Main reason for delay				
Neutropenia	27	75.0	80	27.7
Thrombocytopenia	5	13.9	6	2.1
Diarrhea (≥Grade 2 or watery stool)	2	5.6	2	0.7
Total bilirubin (>1.5 mg/dL)	1	2.8	2	0.7
Peripheral sensory neuropathy	1	2.8	1	0.3
Investigator decision	12	33.3	26	9.0
Patient conveniences	7	19.4	10	3.5
Other	5	13.9	5	1.7

†After two cycles.

At the time of analysis, 27 patients had died, 9 patients were alive, and no patients were lost to follow-up.

Of the 36 enrolled patients, 33 received secondary treatment. The most common treatment comprised GEM-based regimens, which were given to 28 patients (GEM, n = 23; GEM plus erlotinib, n = 4; GEM + S-1, n = 1). The other regimens included S-1 alone in two patients, and S-1 plus radiation, and FOLFOX in one patient each. Following the FOLFIRINOX treatment, R0 resection of pathology by distal pancreatectomy and splenectomy was achieved in one patient.

Safety. Grade 3 or 4 toxicities occurred in 31 patients (86.1%). There were no treatment-related deaths. The major grade 3 and 4 toxicities are listed in Table 4. The major grade 3 or 4 hematological toxicities were neutropenia (77.8%), leucopenia (44.4%), febrile neutropenia (22.2%), thrombocytopenia (11.1%), and anemia (11.1%). Neutropenia and febrile neutropenia occurred frequently, and 52.8% of the patients were treated with G-CSF to control these toxicities. The incidence of neutropenia decreased as the number of cycles increased (Table 5), and febrile neutropenia occurred only during the first cycle.

The major grade 3 and 4 non-hematological toxicities were anorexia (11.1%), diarrhea (8.3%), nausea (8.3%), an increased alanine transaminase level (8.3%), and peripheral sensory neuropathy (5.6%). No grade 3 or 4 fatigue or vomiting was reported. Cholinergic syndrome, an irinotecan-specific toxicity, was observed in 33% of the patients, but was resolved immediately after treatment with atropine or butylscopolamine.

Serious adverse events occurred in 12 patients (33.3%), and treatment-related toxicity occurred in nine patients (25.0%), including febrile neutropenia in three patients (8.3%) and infection in two patients (5.6%). Severe infection identified as sepsis was observed in two patients, during the 10th and 17th cycle of the treatment, respectively. The infection recovered to grade 1 by the end of the cycle in one patient, however, the treatment had to be discontinued due to concurrent liver abscess. The infection recovered to grade 0 in the other patient by the end of the cycle, however, the treatment was discontinued due to concurrent cholangitis. In terms of SAEs, biliary tract-related events were reported in five patients, including cholangitis, obstructive jaundice, biliary tract infection, and an increased level of blood bilirubin in two, one, one, and two

Table 3. Efficacy results in chemotherapy-naïve Japanese patients with metastatic pancreatic cancer treated with FOLFIRINOX (n = 36)

Best overall response	*N*	%
CR	0	0
PR	14	38.9
SD	11	30.6
Progressive disease	10	27.8
Not evaluated	1	2.8
Response rate (CR+PR)	14	38.9
Disease control rate (CR+PR+SD)	25	69.4
Median time to PR, days†	49	
n†	16	
95% confidence interval†	42.0–77.0	
Range†	35–129	
Median duration of overall response, days‡	170	
n‡	14	
95% confidence interval‡	156.0–196.0	
Range‡	42–287	

†Including patients with partial response (PR). ‡Including patients with PR as best response. CR, complete response; SD, stable disease.

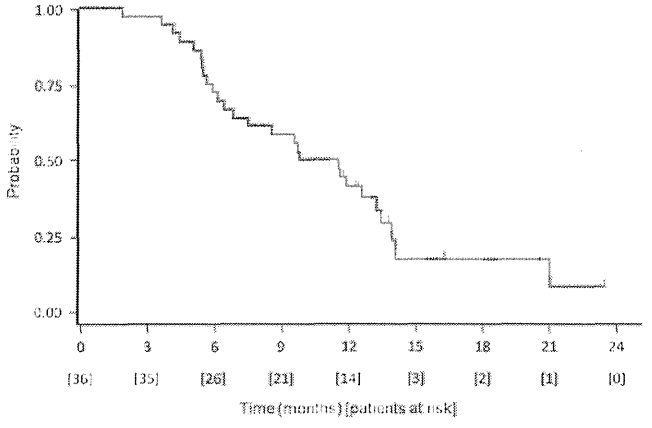

Fig. 1. Kaplan–Meier analysis of overall survival in a phase II study of FOLFIRINOX for chemotherapy-naïve Japanese patients with metastatic pancreatic cancer. The median survival was 10.7 months (95% confidence interval, 6.9–13.2). One-year overall survival was 41.5% (95% confidence interval, 25.4–56.8). Data on nine patients were censored.

patients, respectively, all of which were unrelated to the study treatment.

For patients with or without a biliary stent, febrile neutropenia was observed in 50.0% and 16.7%, biliary tract-related events were observed in 50.0% and 6.7%, and sepsis was observed in 33.3% and 0.0%, respectively.

Discussion

This study was carried out to investigate the efficacy and safety of the FOLFIRINOX regimen in chemotherapy-naïve Japanese patients with MPC. Compared to the FOLFIRINOX phase II/III study by Conroy *et al.*[6] in 2011, the proportion of patients with a PS 0 was high (58.3% *vs* 37.4%) and the proportion of patients in whom the primary site was the pancreatic head was low (19.4% *vs* 39.2%) in this study. However, the proportion of patients with stents at baseline was similar in the two studies (16.7% in this study and 15.8% in the FOLFIRINOX phase II/III study),[6] with no particular differences in other demographic or clinical variables. It is not considered that these small differences in patients' background might compromise comparability in the RR, the primary endpoint of this study, between these two studies.

In the present study, RR, which was the primary endpoint, was 38.9% (95% CI, 23.1–56.5), with the lower limit of the 95% CI being above the threshold RR of 10%. Other efficacy endpoints (PFS, 5.6 months; OS, 10.7 months) were also favorable and were similar to the findings of the FOLFIRINOX

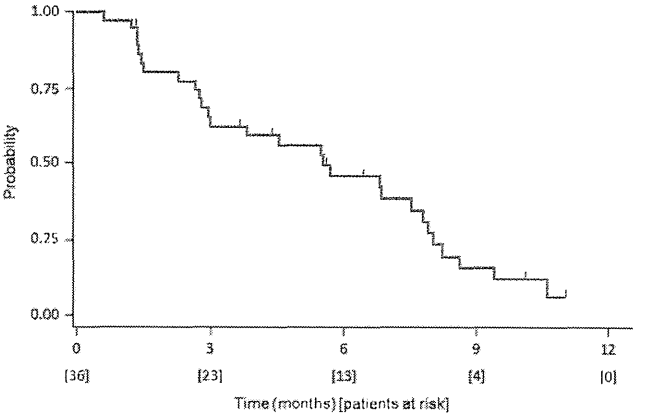

Fig. 2. Kaplan–Meier analysis of progression-free survival in a phase II study of FOLFIRINOX for chemotherapy-naïve Japanese patients with metastatic pancreatic cancer. The median progression-free survival was 5.6 months (95% confidence interval, 3.0–7.8). Data on eight patients were censored.

Table 4. Toxicities in chemotherapy-naïve Japanese patients with metastatic pancreatic cancer treated with FOLFIRINOX (n = 36)

	Any grade		≥Grade 3	
	n	%	*n*	%
Hematological toxicities				
Neutropenia	34	94.4	28	77.8
Febrile neutropenia	8	22.2	8	22.2
Leukopenia	33	91.7	16	44.4
Thrombocytopenia	32	88.9	4	11.1
Anemia	31	86.1	4	11.1
Non-hematological toxicities				
Anorexia	31	86.1	4	11.1
Diarrhea	31	86.1	3	8.3
Nausea	32	88.9	3	8.3
Elevated ALT	20	55.6	3	8.3
Elevated ALP	15	41.7	3	8.3
Elevated GGT	5	13.9	3	8.3
Peripheral sensory neuropathy	27	75.0	2	5.6
Elevated C-reactive protein	24	66.7	2	5.6
Elevated AST	20	55.6	2	5.6
Hypoalbuminaemia	23	63.9	2	5.6
Hypokalaemia	9	25.0	2	5.6
Sepsis	2	5.6	2	5.6

Events listed are those in which grade 3–4 toxicities occurred in more than 5% of patients. ALP, alkaline phosphatase; ALT, alanine aminotransferase; AST, aspartate aminotransferase; GGT, galactolipid galactosyltransferase.

Table 5. Neutropenia by cycle in chemotherapy-naïve Japanese patients with metastatic pancreatic cancer treated with FOLFIRINOX (n = 36)

Cycle	Total patients per cycle (n)	≥Grade 3 neutropenia	
		n	%
Total	36	28	77.8
1	36	24	66.7
2	33	13	39.4
3	30	5	16.7
4	28	5	17.9
5	27	6	22.2
6	24	4	16.7
7	19	1	5.3
8	19	1	5.3

phase II/III study (PFS, 6.4 months; OS, 11.1 months).[6] The results of this study were also favorable compared to those of previous studies of first-line treatment in patients with MPC, including Japanese patients, wherein the OS was 7.0–9.4 months.[7–10] Accordingly, we consider the FOLFIRINOX regimen to be very effective in Japanese patients with pancreatic cancer.

Grade 3–4 neutropenia and febrile neutropenia were more common in this study than those in the FOLFIRINOX phase II/III study (77.8% and 22.2% *vs* 45.7% and 5.4%, respectively).[6] We hypothesize that these discrepancies are due to differences in the laboratory testing frequency, with weekly testing in this study versus testing every 2 weeks in the phase II/III study.

Despite the high incidence of severe neutropenia, febrile neutropenia and infections identified as SAEs were noted in only three and two patients, respectively, in this study. Although febrile neutropenia was observed in eight patients, all of these patients recovered quickly (median recovery time, 2.5 days; range, 2–4) under the appropriate supportive care. In addition, the incidence of neutropenia decreased along with the number of cycles, and febrile neutropenia occurred only in the first cycle. On the basis of these findings, it is considered that active management, including hospitalization, frequent laboratory testing, supportive care for toxicity, and appropriate dose modifications during the treatment period is important, especially during the initial period.

With regard to non-hematological toxicities, the incidences of grade 3 or higher fatigue, vomiting, diarrhea, and peripheral sensory neuropathy were lower in this study than in the FOLFIRINOX phase II/III study (0.0%, 0.0%, 8.3%, and 5.6% *vs* 23.6%, 14.5%, 12.7% and 9.0%, respectively).[6] It is speculated that the lower incidence of vomiting might be associated with the implementation of active prophylactic supportive therapy, including the use of selective neurokinin 1 receptor antagonistic antiemetics in 34 patients in this study.

As anticipated, biliary tract-related events, severe infection, and febrile neutropenia frequently occurred in patients with biliary stents at baseline, indicating that careful management is required in these patients to avoid the development of cholangitis or infection.

In this study, patients homozygous for *UGT1A1*28* or *UGT1A1*6* or heterozygous for both *UGT1A1*6* and *UGT1A1*28* were excluded. *UGT1A1* is involved in the metabolism of SN-38, an active metabolite of irinotecan, and variants of *UGT1A1* have been reported to intensify myelosuppression, such as severe neutropenia.[11–13] The efficacy and safety of FOLFIRINOX have not yet been evaluated in patients homozygous for *UGT1A1*28* or *UGT1A1*6* or heterozygous for both *UGT1A1*6* and *UGT1A1*28* in Japan; genetic polymorphism was not included in the eligibility of the phase III trial of FOLFIRINOX. Considering the high incidence of neutropenia in this study, indication of FOLFIRINOX and intensive follow-up for these patients should be considered carefully, especially in Japan.

In 2013, combination therapy of nab-paclitaxel and GEM was found to prolong the survival of patients with MPC compared to GEM alone (the MPACT study).[14] The RR, median OS, and median PFS associated with nab-paclitaxel plus GEM were 23%, 8.5, and 5.5 months, respectively, indicating that this may represent another prospective regimen for patients with MPC. However, no randomized controlled study has yet been carried out to compare FOLFIRINOX and nab-paclitaxel plus GEM.

Because of the severe toxicity of FOLFIRINOX, it cannot be applied to all patients with metastatic pancreatic cancer as a standard of care. At present, the choice of regimen, whether FOLFIRINOX or GEM-based chemotherapy, depends on general conditions in each patient, and FOLFIRINOX is generally recommended to the patients who fulfill the eligibility criteria of this study. Recently, several clinical studies of a modified FOLFIRINOX regimen have been carried out to reduce its toxicities.[15,16] The FOLFIRINOX regimen is also investigated in patients with genetic polymorphisms of *UGT1A1*28* or **6*, which were excluded in this study.[17] As it is important to select the most appropriate treatment regimen based on the clinical information of the patients, these results may provide a guide to selection for each individual patient.

In conclusion, on the basis of our findings in this study, the FOLFIRINOX regimen appears to be effective in Japanese patients, and the associated toxicity can be adequately controlled by careful observation and appropriate supportive care. Thus, FOLFIRINOX can be the standard treatment for Japanese patients with MPC with good performance status (ECOG PS 0 or 1) and normal bilirubin level.

Acknowledgments

This study was supported by Yakult Honsha Co., Ltd. We thank all patients, clinicians, and support staff who participated in this study. We are grateful to Yuh Sakata, Ichinosuke Hyodo, and Fumitaka Nagamura for their helpful advice as members of the Independent Data Monitoring Committee, and Atsushi Sato, Kunihisa Miyakawa, and Kouki Yoshikawa as members of the Independent Review Committee. We also thank Noriko Miwa for her helpful advice.

Disclosure Statement

Takuji Okusaka received research grants from Yakult Honsha and Kyowa Hakko Kirin; he has also received honoraria from Pfizer. Akira Fukutomi and Junji Furuse received honoraria from Yakult Honsha. Hiroyuki Isayama and Narikazu Boku received honoraria from Yakult Honsha and Daiichi Sankyo. Masafumi Ikeda, Tatsuya Ioka, and Shinichi Ohkawa have no conflict of interest.

Abbreviations

5-FU	fluorouracil
CI	confidence interval
FAS	full analysis set
FOLFIRINOX	oxaliplatin, irinotecan, fluorouracil, and leucovorin
G-CSF	granulocyte-colony stimulating factor
GEM	gemcitabine

IDMC	Independent Data Monitoring Committee
MPC	metastatic pancreatic cancer
nab-paclitaxel	albumin-bound paclitaxel
OS	overall survival
PFS	progression-free survival
PS	performance status
RR	response rate
SAE	serious adverse events
SD	stable disease
UGT	uridine diphosphate-glucuronosyltransferase

References

1 Jemal A, Bray F, Center MM, Ferlay J, Ward E, Forman D. Global cancer statistics. *CA Cancer J Clin* 2011; **61**: 69–90.
2 Japanese Ministry of Health, Labour and Welfare. Statistical investigation result. 2012: [cited 27 November 2013] Available from URL: http://www.mhlw.go.jp/toukei/saikin/hw/jinkou/kakutei12/index.html [In Japanese]
3 Center for Cancer control and Information Services, Latest Cancer Statistics. [cited 21 November 2013] Available from URL: http://ganjoho.jp/public/statistics/pub/statistics01.html [In Japanese]
4 Burris HA III, Moore MJ, Anderson J *et al.* Improvements in survival and clinical benefit with gemcitabine as first-line therapy for patients with advanced pancreas cancer: a randomized trial. *J Clin Oncol* 1997; **15**: 2403–13.
5 Moore MJ, Goldstein D, Hamm J *et al.* Erlotnib plus gemcitabine compared with gemcitabine alone in patients with advanced pancreatic cancer: a phase III trial of the national cancer instutite of Canada Clinical Trials Group. *J Clin Oncol* 2007; **25**: 1960–6.
6 Conroy T, Desseigne F, Ychou M *et al.* FOLFIRINOX versus gemcitabine for metastatic pancreas cancer. *N Engl J Med* 2011; **364**: 1817–25.
7 Ueno H, Okusaka T, Funakoshi A *et al.* A phase II study of weekly irinotecan as first-line therapy for patients with metastatic pancreatic cancer. *Cancer Chemother Pharmacol* 2007; **59**: 447–54.
8 Okusaka T, Funakoshi A, Furuse J *et al.* A late phase II study of S-1 for metastatic pancreatic cancer. *Cancer Chemother Pharmacol* 2008; **61**: 615–21.
9 Kindler HL, Ioka T, Richel DJ *et al.* Axitnib plus gemcitabinc versus placebo plus gemcitabine in patients with advanced pancreatic adenocarcinoma: a double-blind randomized phase 3 study. *Lancet Oncol* 2011; **12**: 256–62.
10 Ueno H, Ioka T, Ikeda M *et al.* Randomized phase III study of gemcitabine plus S-1, S-1 alone, or gemcitabine alone in patients with locally advanced and metastatic pancreatic cancer in Japan and Taiwan: GEST study. *J Clin Oncol* 2013; **31**: 1640–8.
11 Ando Y, Saka H, Ando M *et al.* Polymorphisms of UDP-glucuronosyltransferase gene and irinotecan toxicity: a pharmacogenetic analysis. *Cancer Res* 2000; **60**: 6921–6.
12 Innocenti F, Undevia SD, Iyer L *et al.* Genetic variants in the UDP-glucuronosyltransferase 1A1 gene predict the risk of severe neutropenia of irinotecan. *J Clin Oncol* 2004; **22**: 1382–8.
13 Marcuello E, Altes A, Menoyo A *et al.* UGT1A1 gene variations and irinotecan treatment in patients with metastatic colorectal cancer. *Br J Cancer* 2004; **91**: 678–82.
14 Von Hoff DD, Ervin T, Arena PF *et al.* Increased survival in pancreatic cancer with nab-paclitaxel plus gemcitabine. *N Engl J Med* 2013; **369**: 1691–703.
15 Mahaseth H, Brutcher E, Kauh J *et al.* Modified FOLFIRINOX regimen with improved safety and maintained efficacy in pancreatic adenocarcinoma. *Pancreas* 2013; **42**: 1311–5.
16 Oikonomopoulos GM, Syrigos KN, Skoura E, Saif MW. FOLFIRINOX: from the ACCORD study to 2014. *JOP* 2014; **15**: 103–5.
17 Sharma M, Catenacci DV, Karrison T *et al.* A UGT1A1 genotype guided dosing study of modified FOLFIRINOX (mFOLFIRINOX) in previously untreated patients (pts) with advanced gastrointestinal malignancies. *J Clin Oncol* 2014; **32**(Suppl): 4125.

Supporting Information

Additional supporting information may be found in the online version of this article:

Table S1. Dose level at dose adjustment in chemotherapy-naïve Japanese patients with metastatic pancreatic cancer treated with FOLFIRINOX (n = 36).

Table S2. Dose adjustment criteria in hematological toxicity in chemotherapy-naïve Japanese patients with metastatic pancreatic cancer treated with FOLFIRINOX (n = 36).

Table S3. Dose adjustment criteria in non-hematological toxicity in chemotherapy-naïve.

European Journal of Cancer (2014) 50, 1900–1908

Available at www.sciencedirect.com

ScienceDirect

journal homepage: www.ejcancer.com

Prognostic impact of M2 macrophages at neural invasion in patients with invasive ductal carcinoma of the pancreas

Motokazu Sugimoto [a,b,d], Shuichi Mitsunaga [a,c], Kiyoshi Yoshikawa [a], Yuichiro Kato [b], Naoto Gotohda [b], Shinichiro Takahashi [b], Masaru Konishi [b], Masafumi Ikeda [c], Motohiro Kojima [a], Atsushi Ochiai [a,*], Hironori Kaneko [d]

[a] *Division of Pathology, Research Center for Innovative Oncology, National Cancer Center Hospital East, Japan*
[b] *Department of Hepatobiliary and Pancreatic Surgery, National Cancer Center Hospital East, Japan*
[c] *Department of Hepatobiliary and Pancreatic Oncology, National Cancer Center Hospital East, Japan*
[d] *Department of Surgery, Toho University School of Medicine, Japan*

Received 11 March 2014; accepted 9 April 2014
Available online 15 May 2014

KEYWORDS
Pancreatic cancer
Pancreaticoduodenectomy
Neural invasion
M2 macrophages
Overall survival
Peritoneal dissemination
Locoregional recurrence
Adjuvant chemotherapy

Abstract ***Background:*** Neural invasion is a characteristic pattern of invasion and an important prognostic factor for invasive ductal carcinoma (IDC) of the pancreas. M2 macrophages have reportedly been associated with poor prognosis in various cancers. The aim of the present study was to investigate the prognostic impact of M2 macrophages at extrapancreatic nerve plexus invasion (plx-inv) of pancreatic IDC.

Methods: Participants comprised 170 patients who underwent curative pancreaticoduodenectomy for pancreatic IDC. Immunohistochemical examination of surgical specimens was performed by using CD204 as an M2 macrophage marker, and the area of immunopositive cells was calculated automatically. Prognostic analyses of clinicopathological factors including CD204-positive cells at plx-inv were performed.

Results: Plx-inv was observed in 91 patients (53.5%). Forty-eight patients showed a high percentage of CD204-positive cell area at plx-inv (plx-inv CD204%^{high}). Plx-inv CD204%^{high} was an independent predictor of poor outcomes for overall survival (OS) ($P < 0.001$) and disease-free survival (DFS) ($P < 0.001$). Patients with plx-inv CD204%^{high} showed a shorter time to peritoneal dissemination ($P < 0.001$) and locoregonal recurrence ($P < 0.001$). In patients who underwent adjuvant chemotherapy, plx-inv CD204%^{high} was correlated with shorter OS ($P = 0.011$) and DFS ($P = 0.038$) in multivariate analysis.

* *Corresponding author:* Address: National Cancer Center Hospital East, 6-5-1 Kashiwa-no-ha, Kashiwa, Chiba 277-8577, Japan. Tel.: +81 4 7134 6855; fax: +81 4 7134 6865.
E-mail address: aochiai@east.ncc.go.jp (A. Ochiai).

http://dx.doi.org/10.1016/j.ejca.2014.04.010